

AD-A246 300



2

NAVAL POSTGRADUATE SCHOOL

Monterey, California



S DTIC
ELECTE
FEB 18 1992
D

THESIS

PERFORMANCE ENHANCEMENT OF THE NPS TRANSIENT
ELECTROMAGNETIC SCATTERING LABORATORY

by

Aldo E. Bresani

September 1991

Thesis Advisor:

Michael A. Morgan

Approved for public release; distribution is unlimited

92 2 12 132

92-03674



REPORT DOCUMENTATION PAGE			
1a REPORT SECURITY CLASSIFICATION UNCLASSIFIED		1b RESTRICTIVE MARKINGS	
2a SECURITY CLASSIFICATION AUTHORITY		3 DISTRIBUTION AVAILABILITY OF REPORT Approved for public release; distribution is unlimited.	
2b DECLASSIFICATION/DOWNGRADING SCHEDULE			
4 PERFORMING ORGANIZATION REPORT NUMBER(S)		5 MONITORING ORGANIZATION REPORT NUMBER(S)	
6a NAME OF PERFORMING ORGANIZATION Naval Postgraduate School	6b OFFICE SYMBOL (If applicable) EC	7a NAME OF MONITORING ORGANIZATION Naval Postgraduate School	
6c ADDRESS (City, State, and ZIP Code) Monterey, CA 93943-5000		7b ADDRESS (City, State, and ZIP Code) Monterey, CA 93943-5000	
8a NAME OF FUNDING/SPONSORING ORGANIZATION	8b OFFICE SYMBOL (If applicable)	9 PROCUREMENT INSTRUMENT IDENTIFICATION NUMBER	
8c ADDRESS (City, State, and ZIP Code)		10 SOURCE OF FUNDING NUMBERS	
		Program Element No	Project No
		Task No	Work Unit Accession Number
11 TITLE (Include Security Classification) PERFORMANCE ENHANCEMENT OF THE NPS TRANSIENT ELECTROMAGNETIC SCATTERING LABORATORY			
12 PERSONAL AUTHOR(S) Bresani, Aldo E.			
13a TYPE OF REPORT Master's Thesis	13b TIME COVERED From To	14 DATE OF REPORT (year, month, day) 1991 September	15 PAGE COUNT 104
16 SUPPLEMENTARY NOTATION The views expressed in this thesis are those of the author and do not reflect the official policy or position of the Department of Defense or the U.S. Government.			
17. COSATI CODES		18. SUBJECT TERMS (continue on reverse if necessary and identify by block number)	
FIELD	GROUP	SUBGROUP	
		Transient Scattering, Signature	
19. ABSTRACT (continue on reverse if necessary and identify by block number)			
<p>This thesis describes the performance enhancement of the NPS Transient Electromagnetic Scattering Laboratory (TESL) accomplished by replacing the old HP 8349A microwave preamplifier of the dual amplifier configuration with a new Avantek 13533 5-13 GHz amplifier and optimizing the delay line length for the 1-6 GHz amplifier. New Matlab software was developed to process the signals scattered from canonical and complex targets. This software includes a program to calculate the correct delay line length for either amplifier in future modifications. The updated TESL is shown to provide measurements yielding excellent agreement with theoretically predicted responses of canonical targets demonstrating a significant improvement of the signal to noise ratio as compared with the previous configuration. A target library was created to support research in radar target identification based on natural resonances.</p>			
20 DISTRIBUTION/AVAILABILITY OF ABSTRACT <input checked="" type="checkbox"/> UNCLASSIFIED/UNLIMITED <input type="checkbox"/> SAME AS REPORT <input type="checkbox"/> DTIC USERS		21. ABSTRACT SECURITY CLASSIFICATION UNCLASSIFIED	
22a NAME OF RESPONSIBLE INDIVIDUAL Morgan, Michael A.		22b TELEPHONE (Include Area code) 408-646-2081	22c. OFFICE SYMBOL EC/Mw

Approved for public release; distribution is unlimited.

PERFORMANCE ENHANCEMENT OF THE NPS TRANSIENT ELECTROMAGNETIC
SCATTERING LABORATORY

by

Aldo E. Bresani
Lieutenant, Peruvian Navy
Peruvian Naval Academy, 1983

Submitted in partial fulfillment
of the requirements for the degrees of

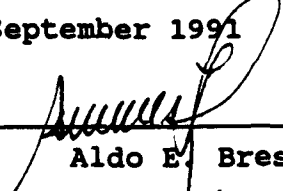
MASTER OF SCIENCE IN ELECTRICAL ENGINEERING
MASTER OF SCIENCE IN SYSTEMS ENGINEERING
(ELECTRONIC WARFARE)

from

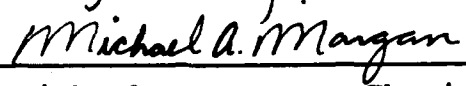
NAVAL POSTGRADUATE SCHOOL

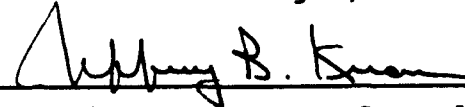
September 1991

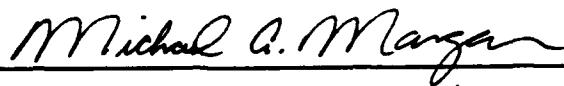
Author:

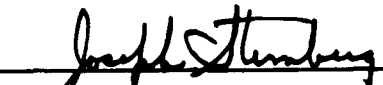

Aldo E. Bresani

Approved by:


Michael A. Morgan, Thesis Advisor


Jeffrey B. Knorr, Second Reader


Michael A. Morgan, Chairman,
Department of Electrical & Computer Engineering


Joseph Sternberg, Chairman,
Electronic Warfare Academic Group

ABSTRACT

This thesis describes the performance enhancement of the NPS Transient Electromagnetic Scattering Laboratory (TESL) accomplished by replacing the old HP 8349A microwave preamplifier of the dual amplifier configuration with a new Avantek 13533 5-13 GHz amplifier and optimizing the delay line length for the 1-6 GHz amplifier. New Matlab software was developed to process the signals scattered from canonical and complex targets. This software includes a program to calculate the correct delay line length for either amplifier in future modifications. The updated TESL is shown to provide measurements yielding excellent agreement with theoretically predicted responses of canonical targets demonstrating a significant improvement of the signal to noise ratio as compared with the previous configuration. A target library was created to support research in radar target identification based on natural resonances.



Accession For	
NTIS CRA&I	<input checked="" type="checkbox"/>
DTIC TAB	<input type="checkbox"/>
Unannounced	<input type="checkbox"/>
Justification	
By	
Distribution /	
Availability Codes	
Dist	Avail. and/or Special
A-1	

TABLE OF CONTENTS

I. INTRODUCTION	1
A. HISTORY OF THE TESL	1
B. OVERVIEW	2
II. LABORATORY DESCRIPTION AND MODIFICATIONS	5
A. LABORATORY DESCRIPTION	5
B. MODIFICATIONS	10
III. THEORY OF TRANSIENT SCATTERING MEASUREMENTS	11
A. TESL SYSTEM REPRESENTATION	13
B. MATHEMATICAL MODEL	15
C. TRANSIENT RESPONSE EVALUATION	17
IV. MEASUREMENT PROCESS AND SIGNAL PROCESSING	20
A. DATA ACQUISITION	20
B. DECONVOLUTION ALGORITHM	21
1. Frequency Domain Deconvolution	22
2. Time Domain Deconvolution	46
C. SYSTEM VALIDATION	51
D. NOISE PERFORMANCE AND SPECTRUM	58
E. SIGNAL TO NOISE RATIO	64

F. TARGET LIBRARY	65
V. CONCLUSIONS	70
A. SUMMARY	70
B. FUTURE CONSIDERATIONS	71
APPENDIX A. TIME AND FREQUENCY DOMAIN DECONVOLUTION PROGRAM	73
APPENDIX B. DELAY LINE SIMULATION PROGRAM	79
APPENDIX C. SNR AND NOISE SPECTRUM PROGRAM	85
APPENDIX D. NOISE PERFORMANCE PROGRAM	89
LIST OF REFERENCES	92
INITIAL DISTRIBUTION LIST	93

LIST OF TABLES

Table 1. SYSTEM REPRESENTATION TRANSFER FUNCTION.....14
Table 2. NUMERICAL COMPUTATION INPUTS OF MIE PROGRAM.....52
Table 3. NUMERICAL COMPUTATION INPUTS OF TSCT PROGRAM.....52
Table 4. NUMERICAL COMPUTATION INPUTS OF TDIE-DG PROGRAM...53
Table 5. AIRCRAFT FULL SIZE DIMENSIONS.....67

LIST OF FIGURES

Figure 1. Interior of Anechoic Chamber.....	6
Figure 2. NPS TESL General Layout.....	7
Figure 3. Exterior Hardware Components.....	8
Figure 4. New Amplifier Configuration.....	9
Figure 5. Amplifier and Antenna Configuration.....	12
Figure 6. TESL System Representation.....	13
Figure 7. Calibration Measurement with Minimum Delay Line (13.5cm).....	23
Figure 8. Calibration Measurement with 25.5 cm Delay Line..	24
Figure 9. Calibration Spectrum with Minimum Delay.....	25
Figure 10. Calibration Spectrum with 25.5 cm Delay Line.....	26
Figure 11. 4" Thin Wire Broadside Measurement with Minimum Delay Line (13.5 cm).....	28
Figure 12. 4" Thin Wire Broadside Measurement with 25.5 cm Delay Line.....	29
Figure 13. 4" Thin Wire Broadside Spectrum with Minimum Delay.....	30
Figure 14. 4" Thin Wire Broadside Spectrum with 25.5 cm Delay Line.....	31
Figure 15. Time and Frequency Domain Plots for the Theoretically Computed Calibration Sphere.....	32
Figure 16. Deconvolution Component with Minimum Delay Line..	33
Figure 17. Deconvolution Component with 25.5 cm Delay Line..	34
Figure 18. 4" Thin Wire Broadside Deconvolution Spectrum with Minimum Delay Line.....	36
Figure 19. 4" Thin Wire Broadside Deconvolution Spectrum with 25.5 cm Delay Line.....	37
Figure 20. 4" Thin Wire Broadside Deconvolved Field with Minimum Delay Line.....	38

Figure 21. 4" Thin Wire Broadside Deconvolved Field with 25.5 cm Delay Line.....	39
Figure 22. 4" Thin Wire Broadside Deconvolved Field with a Simulated 35.5 cm Delay Line.....	44
Figure 23. 4" Thin Wire Broadside Deconvolution Spectrum with a Simulated 35.5 cm Delay Line.....	45
Figure 24. Computed Calibration Sphere and 4" Thin Wire Broadside Deconvolved Impulse Response with Minimum Delay Line.....	47
Figure 25. Computed Calibration Sphere and 4" Thin Wire Broadside Deconvolved Impulse Response with 25.5 cm Delay Line.....	48
Figure 26. 4" Thin Wire Broadside Hybrid Deconvolved Field with Minimum Delay Line.....	49
Figure 27. 4" Thin Wire Broadside Hybrid Deconvolved Field with 25.5 cm Delay Line.....	50
Figure 28. 4" Thin Wire Broadside Validation.....	54
Figure 29. 4" Thin Wire 30 Degrees Aspect Validation.....	55
Figure 30. 12 cm Diameter Sphere Validation.....	56
Figure 31. 8 cm Diameter Sphere Validation.....	57
Figure 32. Old and New Configuration Subtracted Calibration Waveforms Considered for Noise Performance.....	59
Figure 33. Old and New Configuration Noise Waveforms.....	60
Figure 34. Unsmoothed Noise Spectrum.....	62
Figure 35. Time Smoothed Noise Spectrum.....	63
Figure 36. Signal and Noise Waveforms.....	66
Figure 37. Comparison of Aircrafts 1, 2, 3 and 4 Nose-on....	68
Figure 38. Comparison of Aircrafts 1, 2, 3 and 4 Broadside..	69

ACKNOWLEDGEMENTS

I wish to thank Professor Michael A. Morgan for his support and guidance throughout the course of this thesis.

This thesis is dedicated to my wife Liliana for her patience and understanding during the time I spent to work on it.

I. INTRODUCTION

A. HISTORY OF THE TESL

Frequency domain techniques have historically been most often employed for electromagnetic analysis. The band-limited impulse response of measured targets was usually obtained by sweeping frequencies over the entire band using a continuous wave source; time domain techniques were seldom used due to hardware limitations. When fast pulse sources and sampling oscilloscopes became available, time domain techniques gave an alternative way to obtain the transient scattering response of measured targets in a shorter time.

The original Transient Electromagnetic Scattering Laboratory (TESL) was initiated in 1980 by Professor M.A. Morgan who has developed it through the years with his thesis students. Hammond [Ref. 1] worked with this laboratory, researching inverse scattering based upon synthesized ramp responses. The original TESL incorporated an outside ground-plane range and was limited to symmetric targets which could be mirror imaged. In 1983 the TESL became operational as an indoor facility located in Spanagel 535. Mariategui [Ref. 2] measured scattering by suspended targets in a shielded anechoic chamber, which eliminated the requirement of target mirror symmetry. This initial free-field

range provided good transient scattering measurements. In 1985 McDaniel [Ref. 3] showed good agreement between theoretical computations and measurements of the impulse responses for a sphere and a thin wire.

In 1988 Sompae [Ref. 4] incorporated new measurement and computational hardware and designed new software to automate high quality transient scattering measurements. The major hardware included a microcomputer, a new HP 54120T digital programmable oscilloscope (DPO), and a shielded anechoic chamber. Automatic transient scattering measurements were performed using an IEEE bus controller. He showed very good results comparing experimental measurements and computations for a sphere and a thin wire. An improvement of 10 dB over the Tektronix hardware previously used was achieved.

Prior to the current effort Walsh [Ref. 5] incorporated two parallel GaAs FET broadband amplifiers to extend the frequency range and improve the signal to noise ratio (SNR) of the TESL. An improvement of up to 8 dB in SNR was observed when compared with the single amplifier configuration.

B. OVERVIEW

The emphasis of this research was to investigate several improvements in the implementation of the dual amplifier configuration for the TESL. Hardware improvements involved

replacing the old HP 8349A 2-20 GHz microwave preamplifier with a new Avantek AWT 13533 5-13 GHz amplifier and optimizing the delay line for the 1-6 GHz amplifier. New Matlab software was developed to make the process more user friendly and more efficient, allowing an in-depth analysis of the measured and processed waveforms. The new software includes a program employing two different approaches: time domain and frequency domain deconvolution. In addition programs to calculate the SNR, noise performance and noise spectrum of the TESL have been developed and tested. Another Matlab program was created for future changes in the TESL in order to calculate the correct delay line length for each of the amplifiers.

Validation of the new configuration was done by comparing experimental results to that theoretically predicted for simple canonical targets. A library of high quality measurements for simple canonical and scale model military targets was created. This library will be used for testing new natural resonance extraction algorithms and resonance annihilation filters as applied to aspect invariant radar target identification.

This thesis is broken into six Chapters. Chapter II describes the physical laboratory facilities and the changes incorporated through this work.

The theory of transient scattering measurements, the mathematical model, and the transient response solution are explained in Chapter III.

The description of the acquisition algorithm and measurement process with examples can be found in Chapter IV. Also in this chapter, one can find a description of Matlab software developed in this thesis. Experimental results compared with theoretical predictions are also displayed, as well as the SNR, noise performance and spectra. Moreover, the target library created is listed in detail in Chapter IV.

Chapter V presents an overall review of the work and some suggested improvements for the TESL.

II. LABORATORY DESCRIPTION AND MODIFICATIONS

A. LABORATORY DESCRIPTION

The anechoic chamber of the Naval Postgraduate School Transient Electromagnetic Scattering Laboratory is located in Spanagel Hall, room 535. It incorporates a metallicly shielded anechoic chamber to avoid outside electromagnetic interference and to provide minimum reflections in order to simulate free space. The dimensions are 6.10 meters long, 3.05 meters height and 3.05 meters width. Targets are measured on a low density styrofoam pedestal, located 2.18 meters from the antenna array panel. The interior (floor, side walls, and ceiling) is covered with longitudinal wedges of a special carbon impregnated foam absorbing material used to direct the energy towards the absorbing back wall. The interior of this chamber is illustrated in Figure 1. Further information describing the chamber can be found in References 2 and 3.

The hardware components of the TESL are the following:

- HP54120T Digital Programmable Oscilloscope (DPO).
- HP54120A Digitizing Oscilloscope Mainframe.
- HP54121A Four Channel Test Set.
- HP-IB Controller Interface.
- AVANTEK SA83-2954 2-6 GHz amplifier.
- AVANTEK APT-12066 6-12 GHz amplifier.

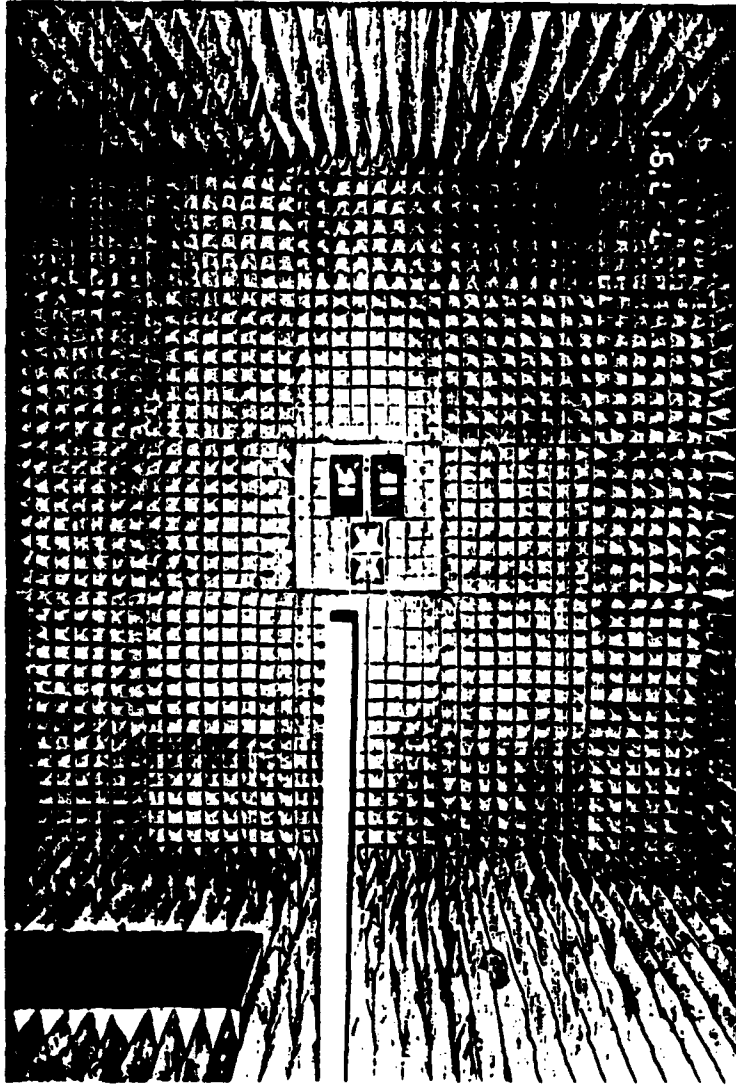


Figure 1. Interior of Anechoic Chamber

- AVANTEK AWT-13533 5-13 GHz preamplifier.
- Midisco inductive power splitter.
- 141 mil semirigid coax cabling.
- Two cooling fans.
- Two transmitting horn antennas.
- One receiving horn antenna.
- PC 80386 25 MHz with 80387 math coprocessor.

Further details about target acquisition software and hardware can be found in References 4 and 5. The exterior hardware components are shown in Figures 3 and 4. The NPS TESL general layout is shown in Figure 2.

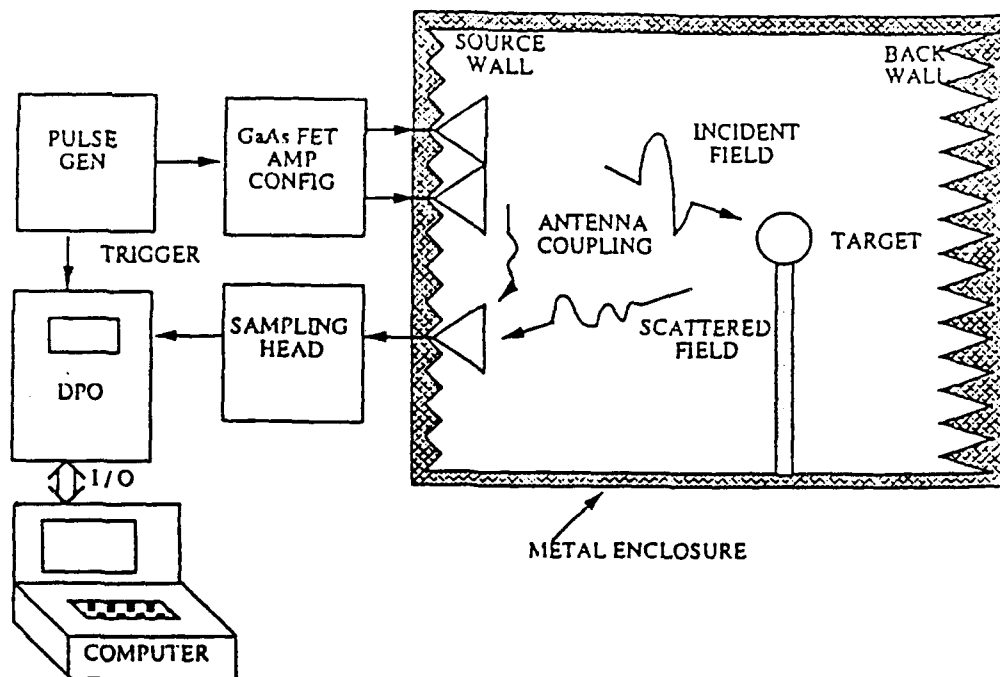


Figure 2. (From Ref. 5) NPS TESL General Layout

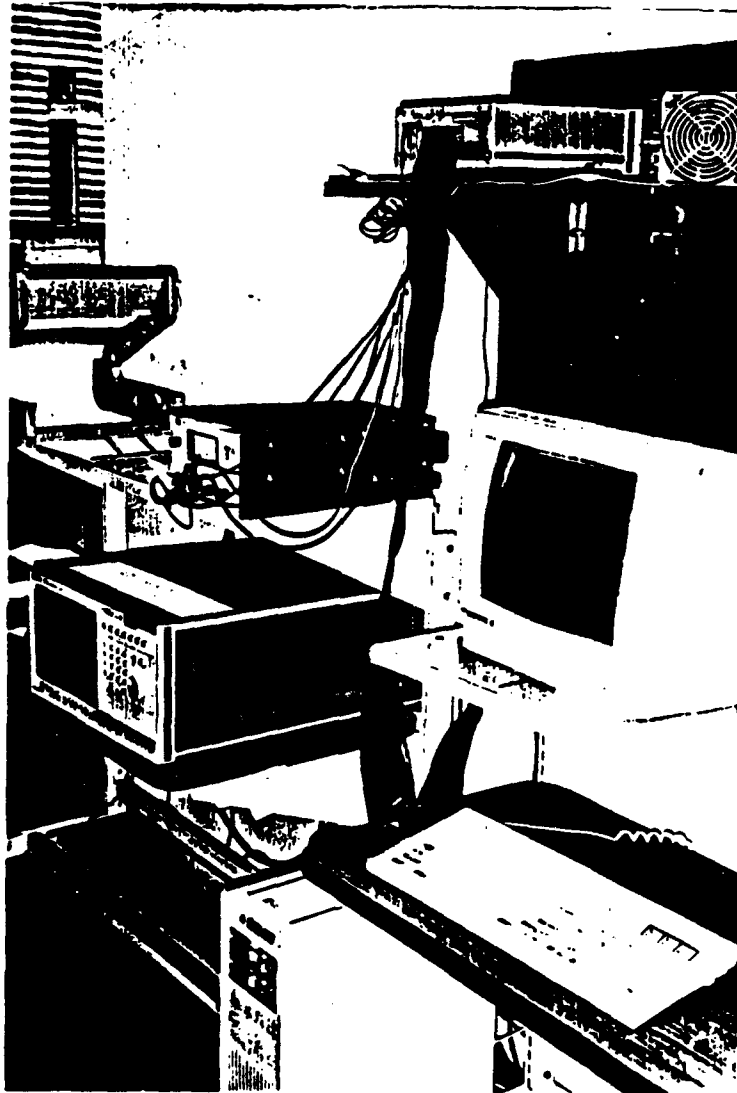


Figure 3. Exterior Hardware Components

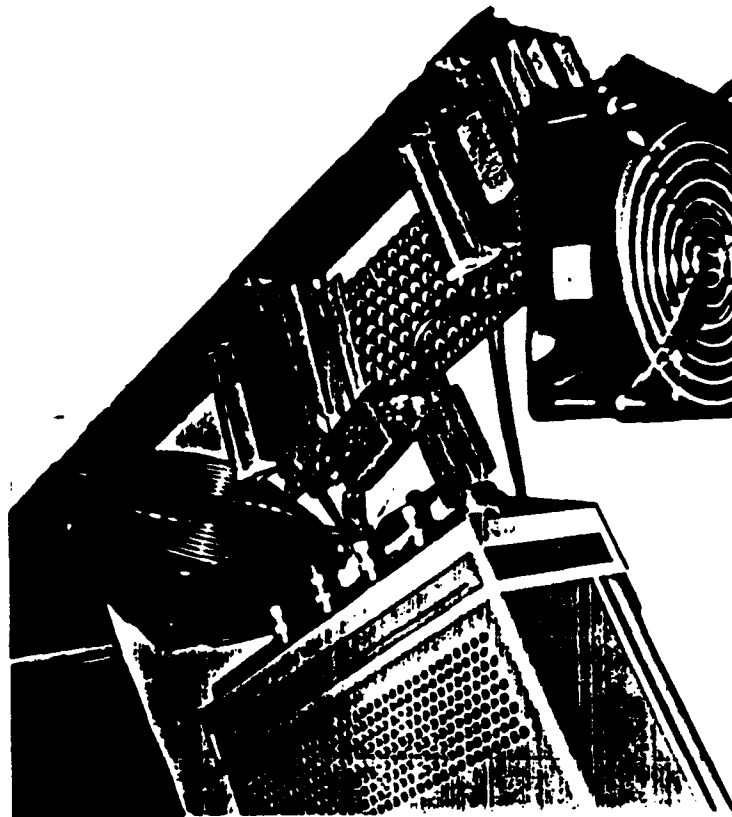


Figure 4. New Amplifier Configuration

B. MODIFICATIONS

The most significant modifications done during this thesis to the TESL were the replacement of the HP 8349A microwave amplifier by an AVANTEK AWT-13533 amplifier, (which is a higher gain lower noise device than the Hewlett Packard), and the delay line for the 2-6 GHz amplifier. The amplifiers and antenna configuration are illustrated in Figure 5.

Walsh [Ref. 5] reported deep nulls in the spectrum due to destructive interference between the waveforms in the area of spectral overlap. For this reason he empirically deduced the correct delay line for the low frequency amplifier using a tedious cut-and-try procedure.

In this new effort initially only the upper band amplifier was changed and the minimum length coaxial line was set up for each of the amplifiers. Once the first measurements were taken and after signal processing, the spectrum did not show any nulls but the time waveform had an oscillation in front of the response. The analysis of this oscillation showed that there was not any problem related to destructive interference. It was thought that the problem was in the signal processing. Several trials, that will be explained in Chapter IV, were done with existing and new software in order to eliminate the undesired oscillation without any success. It was determined that there was not a software problem. A Matlab program was created in order to simulate the effect of the delay line in each one of the amplifiers. Two sets of measurements were

taken, each with just one amplifier in place and the other amplifier replaced by a dummy load. When the program was run, it was determined that the delay line had a large effect in the time domain deconvolution waveform, although the spectrum did not show any deep voids.

Each measured waveform has 1024 points corresponding to a 20 Nsec window, so it was determined that the best results were obtained when the measured waveform from the 2-6 GHz amplifier was delayed 30 time points. This corresponds to 0.56 Nsec. The dielectric constant of the 141 mil semirigid coaxial cable is specified as 2.0006, [Ref 5].

The speed of light inside the coaxial cable is:

$$v = \frac{c}{\sqrt{\epsilon_r}} = \frac{3 \cdot 10^8 \text{ m/s}}{\sqrt{2.0006}} = 2.12 \cdot 10^8 \text{ m/s}$$

where c = speed of light in free space

ϵ_r = dielectric constant of coaxial cable

The extra delay line has length:

$$e = v \cdot \Delta t = 12.01 \text{ cm}$$

The final delay line for the low frequency amplifier was 25.5 cm, which yielded the best results. In Chapter IV typical scattered and measured deconvolution waveforms of different canonical and complex targets are shown, obtained using the minimum coaxial line and with the final extra delay.

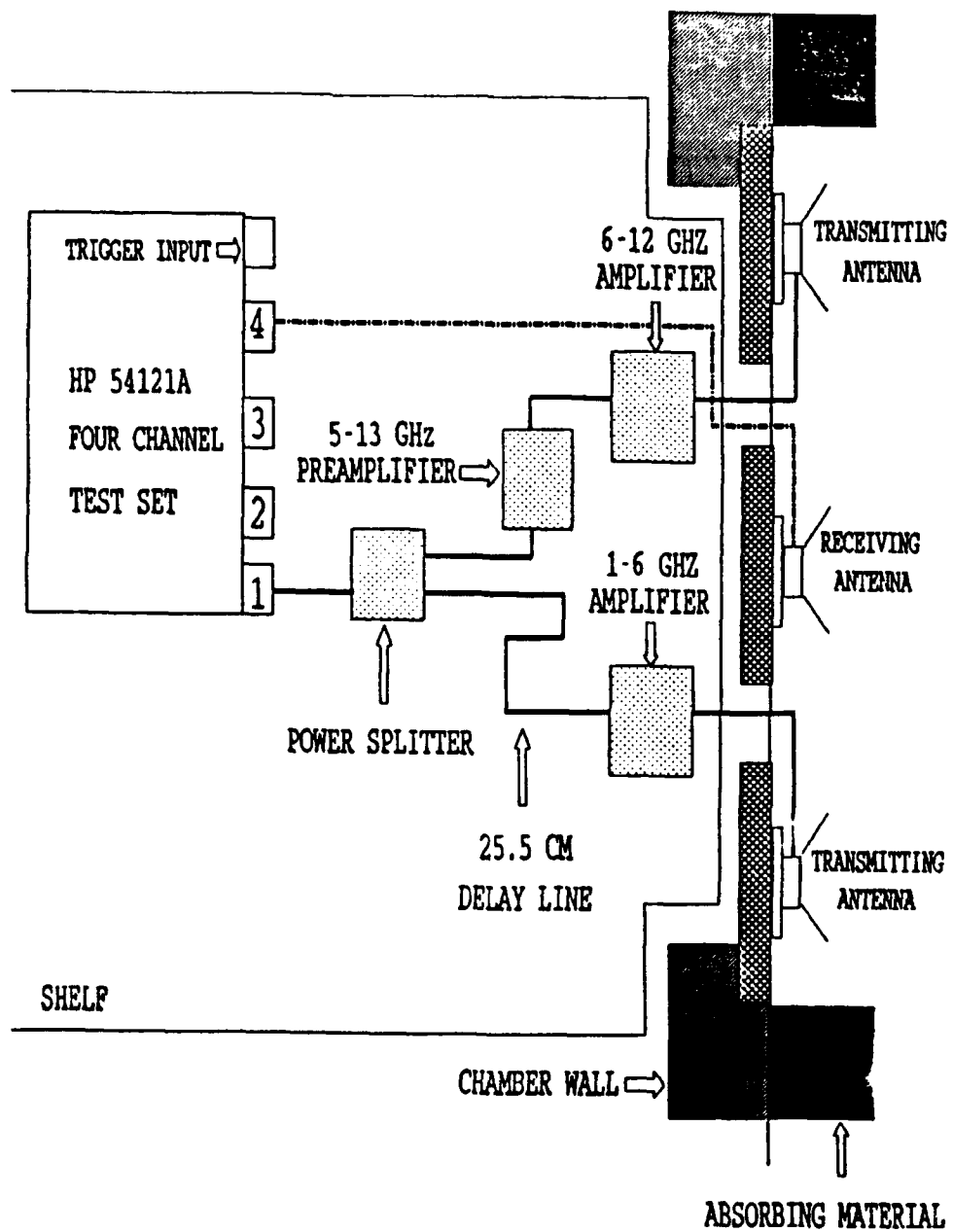


Figure 5. Amplifiers and Antenna Configuration

III. THEORY OF TRANSIENT SCATTERING MEASUREMENTS

A. TESL SYSTEM REPRESENTATION

The Transient Electromagnetic Scattering Laboratory system representation transfer function is illustrated in Figure 6.

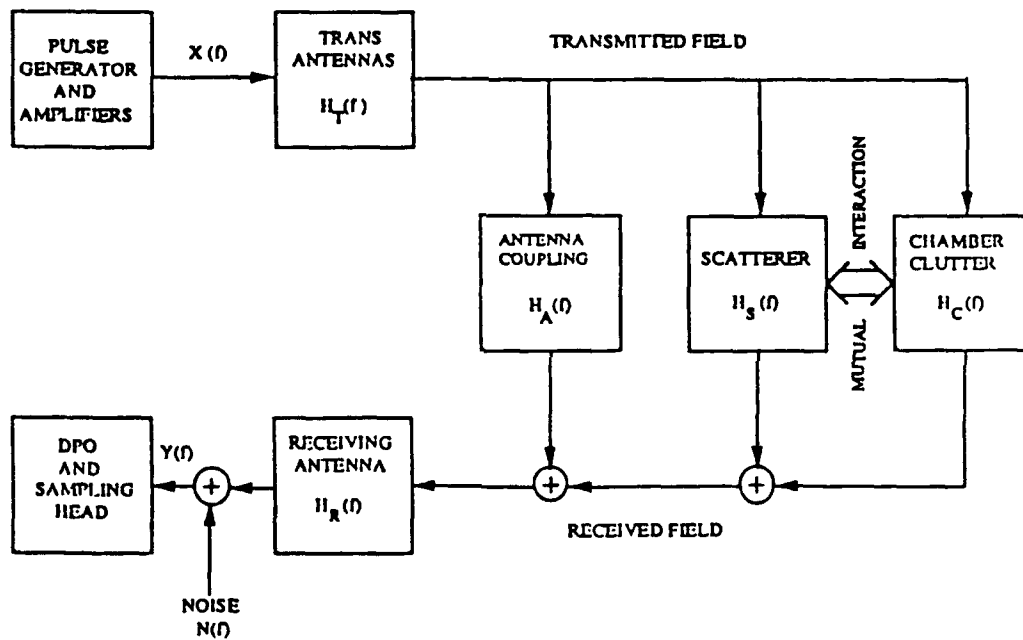


Figure 6. (From Ref. 5) TESL System Representation

The following table specifies the transfer functions used in the system representation and the mathematical model is explained in the next section.

TABLE 1. SYSTEM REPRESENTATION TRANSFER FUNCTIONS

Pulse generator driving the Tx antennas	$X(f)$
Transmitting antennas response	$H_T(f)$
Receiving antenna response	$H_R(f)$
Direct couple of receiving and transmitting antennas	$H_A(f)$
Target response	$H_S(f)$
Chamber response	$H_C(f)$
Interaction between target and chamber	$H_{SC}(f)$
Target measurement	$H_{XS}(f)$
Multiple scattering between target and absorber for target measurement	$H_{XSC}(f)$
Calibration measurement	$H_{YS}(f)$
Multiple scattering between calibration sphere and absorber for calibration measurement	$H_{YSC}(f)$
Total system noise	$N(f)$
Final signal which is sampled	$Y(f)$

In the TESL, the pulse source is the step generator in the Time Domain Reflectometry (TDR) system. This output is available from channel 1 of the HP54121A shown in Figure 3. This sub-assembly is also the coherent trigger for the sampling circuits of the DPO receiver and thus provides exceptional time coherence of the system. The risetime of the step generator is approximately 25 psec and it operates at a 500 KHz repetition frequency.

After the pulse is amplified, it drives the transmitting antennas which radiate into the anechoic chamber. The radiated field couples directly into the receiving antenna, which interacts with the scatterer and the chamber clutter. Multiple scattering between the target and the chamber clutter is indicated by the two-way arrow in Figure 6 on page 13. The total noise of the system is due to the thermal emission inside the chamber and the receiver noise in the sampling front end of the DPO.

B. MATHEMATICAL MODEL

In order to obtain the transfer function of the target, three independent measurements are required. Normally the first is done with a calibration target, which is usually a 15 cm diameter sphere. This is called the calibration measurement. The second is with no target present and is called the background measurement. The third is with the target of interest present and is called the target

measurement. These three measurements can be represented by the transfer functions specified in Table 1.

A calibration measurement is represented as:

$$Y_1(f) = X(f) H_T(f) H_R(f) \{ H_A(f) + H_C(f) + H_{YS}(f) + H_{YSC}(f) \} + N_1(f) \quad (3.1)$$

A background measurement is represented as:

$$Y_2(f) = X(f) H_T(f) H_R(f) \{ H_A(f) + H_C(f) \} + N_2(f) \quad (3.2)$$

A target measurement is represented as:

$$Y_3(f) = X(f) H_T(f) H_R(f) \{ H_A(f) + H_C(f) + H_{XS}(f) + H_{XSC}(f) \} + N_3(f) \quad (3.3)$$

These three equations show that the final signal sampled by the Digital Programmable Oscilloscope is equal to the transfer function product of the amplified pulse, the transmitting antennas and the receiving antenna times the sum of the antenna coupling, the chamber response, the target response and its respective interaction with the chamber. For equation 3.2 the last two transfer functions are not considered since there is no target present. The total noise described before is added to each of these measurements.

C. TRANSIENT RESPONSE EVALUATION

The transient response solution of the measured target, due to a double Gaussian pulse for this work, is obtained by an optimal deconvolution estimator developed by Raid [Ref. 6].

The first step in the process is subtracting the background measurement from the calibration and target measurements, to eliminate the antenna coupling and chamber clutter effects. These subtractions give the following equations:

$$Y_4(f) = Y_1(f) - Y_2(f) \quad (3.4)$$

$$Y_4(f) = X(f)H_T(f)H_R(f)(H_{YS}(f) + H_{YSC}(f)) + N_4(f) \quad (3.5)$$

$$N_4(f) = N_1(f) - N_2(f) \quad (3.6)$$

$$Y_5(f) = Y_3(f) - Y_2(f) \quad (3.7)$$

$$Y_5(f) = X(f)H_T(f)H_R(f)(H_{XS}(f) + H_{XSC}(f)) + N_5(f) \quad (3.8)$$

$$N_5(f) = N_3(f) - N_2(f) \quad (3.9)$$

The time domain subtracted measurements are transformed by the Fast Fourier Transform (FFT) to the frequency domain,

giving $Y_4(f)$ and $Y_5(f)$, and the optimal deconvolution estimator is applied,

$$X_0(f) H_{XS}(f) = \frac{Y_4^*(f) Y_5(f)}{Y_4(f) Y_4^*(f) + C} [X_0(f) H_{VS}(f)] \quad (3.10)$$

where $X_0(f)H_{XS}(f)$ is the target transient response due to the double Gaussian pulse denoted by $x_0(t)$. The smoothing parameter that avoids noise enhancement at frequencies where the spectrum of the subtracted calibration measurement approaches zero is denoted by "C".

The term $X_0(f)H_{VS}(f)$ represents the **computed calibration sphere** response due to the specified pulse waveform illuminating the same size sphere as employed in the calibration measurement. This computed response is obtained by two programs written by M.A. Morgan. The first is programmed in Basic, called **MIE**, which calculates the magnitude and phase of the sphere's transfer function. The second, programmed in Fortran and called **TSCT**, takes the files created in the first and calculates the transient scattering response of the calibration sphere due to an incident double Gaussian pulse.

$$X_0(f) = \mathcal{F} \{ x_0(t) \} \quad (3.11)$$

The double Gaussian pulse waveform used in this thesis is given by:

$$x_0(t) = C_1 e^{-\alpha_1(t-t_0)^2} + C_2 e^{-\alpha_2(t-t_0)^2} \quad (3.12)$$

where C_1 and C_2 are selected to give unit value at t_0 :

$$x_0(t_0) = 1 \quad (3.13)$$

and zero d.c. content,

$$\int_{-\infty}^{\infty} x(t) dt = 0 \quad (3.14)$$

In equation 3.12, the double Gaussian pulse waveform is specified by two 10% pulse widths, Δt_k , such that:

$$e^{-\frac{\alpha_k}{4}(\Delta t_k)^2} = 0.1 \quad \text{for } k=1,2 \quad (3.15)$$

For this work, the narrow pulse width was selected to be 0.15 Nsec and the wide pulse width to be 0.30 Nsec. The reason for these values is that the dual parallel amplifiers, antennas and the DPO configuration, provide an effective 1 to 12.4 GHz passband.

IV. MEASUREMENT PROCESS AND SIGNAL PROCESSING

A. DATA ACQUISITION

The data acquisition in the TESL is accomplished by a program written in Microsoft GW Basic, called ACQU3 [Ref. 4]. The program begins by asking the user if it is a new measurement or if it is desired to use the last data. After this selection a friendly menu is presented on the screen where the user can select the filename for data output, (i.e. calibration, background or target). The number of time points in the acquired waveform is then selected. This has to be a power of two, ranging from 128 to 1024. The third item is the number of subaverages, which also has to be a power of two, ranging from 128 to 2048. In this thesis all the acquired waveforms were selected to be 1024 time points resolution and 2048 subaverages, in a 20 nsec window, to obtain an optimal resolution. The fourth item is the number of data blocks in one record, which normally is one. The eleventh item is the DPO maximum vertical scale which is usually selected to be 16 mV. The last item is the delay time of the scattering signal. This is a very important parameter due to the close proximity of the transmitting and receiving antennas. If no delay time were selected, the direct coupling between antennas would be too large, thus inhibiting scattering observance. The delay

time selected is usually 38 nsec. The four other items not mentioned help to identify the target, waveform type, date and hour of the measurement. When the changes have been completed, the user has to press the letter "R" to be able to run the program. After this step, the user presses the letter "B" to specify the bandwidth to be used. The default bandwidth is 12.4 GHz and the program allows the user to change the default to 20 GHz if desired. Once the 12.4 GHz bandwidth has been specified, the waveform is acquired. The user has to wait until the DPO completes the number of subaverages selected to digitize the data. The acquisition and digitization for 1024 time points and 2048 subaverages takes approximately 30 minutes per waveform.

The ACQU3 program creates a file containing the raw data under the filename selected at the beginning with extension WFM. Further information about the acquisition software can be found in Reference 4.

Next, the user has to edit the files already created by the acquisition program, erase the first four lines of the header and rename the file with extension DAT to use the deconvolution algorithms developed in Matlab.

B. DECONVOLUTION ALGORITHM

The optimal deconvolution algorithm described in Chapter III section C, was initially written by M.A. Morgan for the Tektronis microcomputer [Ref. 2]. When the TESL configuration

was changed and an IBM-AT microcomputer was included, the algorithm was converted to Fortran 77 by Sompaee [Ref. 4].

In this thesis, the algorithm has been converted to Matlab which offers a faster and deeper analysis of the process. Two approaches have been developed which are described in the next subsections.

1. Frequency Domain Deconvolution

The frequency domain deconvolution algorithm (FDDA) uses the optimal deconvolution estimator as it was described in Chapter III, equation 3.10. Once it has been calculated, the inverse FFT is taken to find the scattered field due to a double Gaussian pulse. Typical waveforms of the process will be presented in this subsection, thus comparing the measurements and results obtained by two different delay lines for the low frequency amplifier.

The program begins by asking the filename of the measured calibration sphere waveform (15 cm diameter). The filename entered does not required the extension DAT. Then the program asks for the filename of the measured background for the calibration sphere. After reading each of these files, the time window, number of time points and number of subaverages, will appear on the screen. The program then plots the overlay of the measured waveforms, the subtracted calibration waveform and its spectrum as shown in Figures 7 to 10.

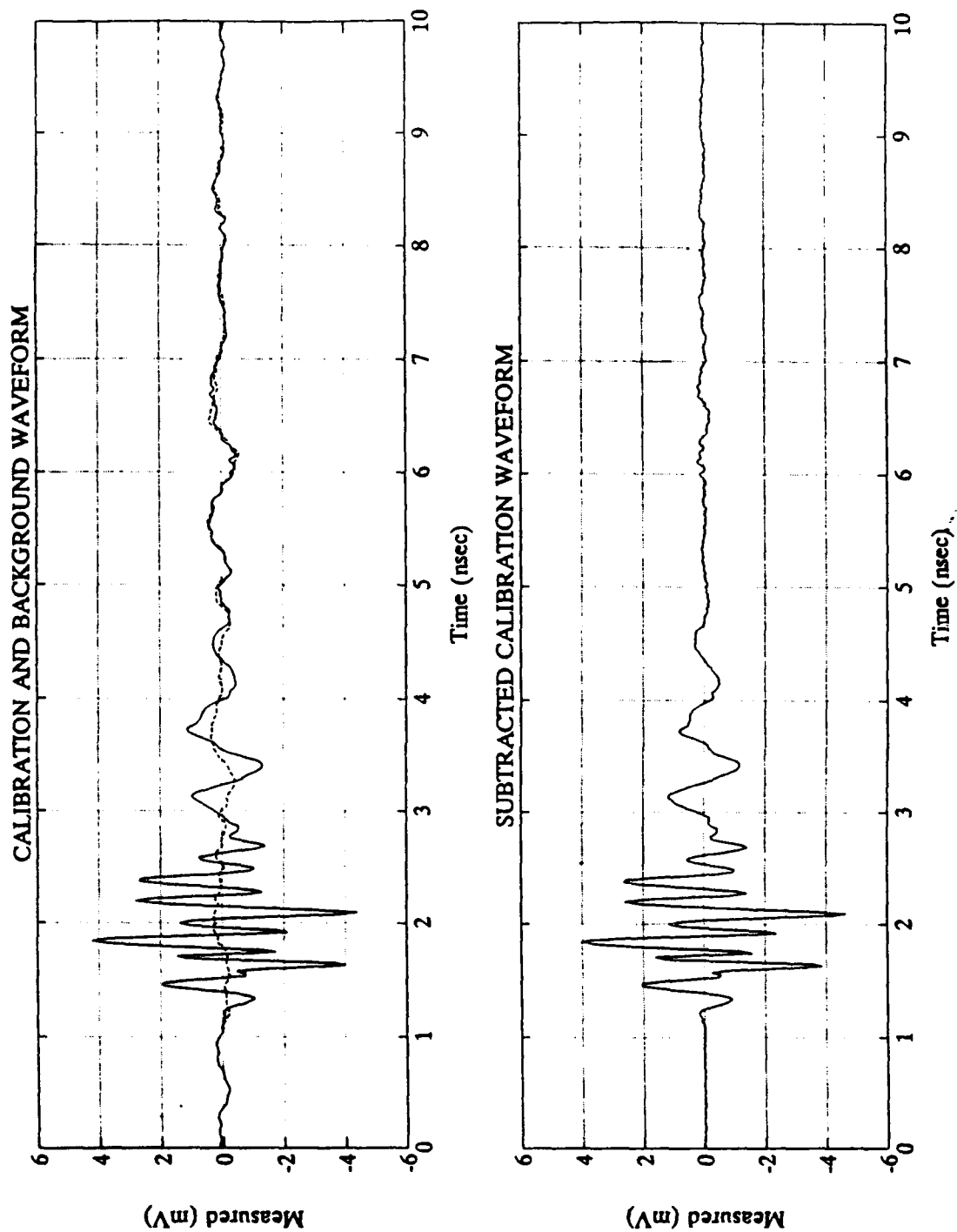


Figure 7. Calibration Measurement with Minimum Delay Line
(13.5 cm)

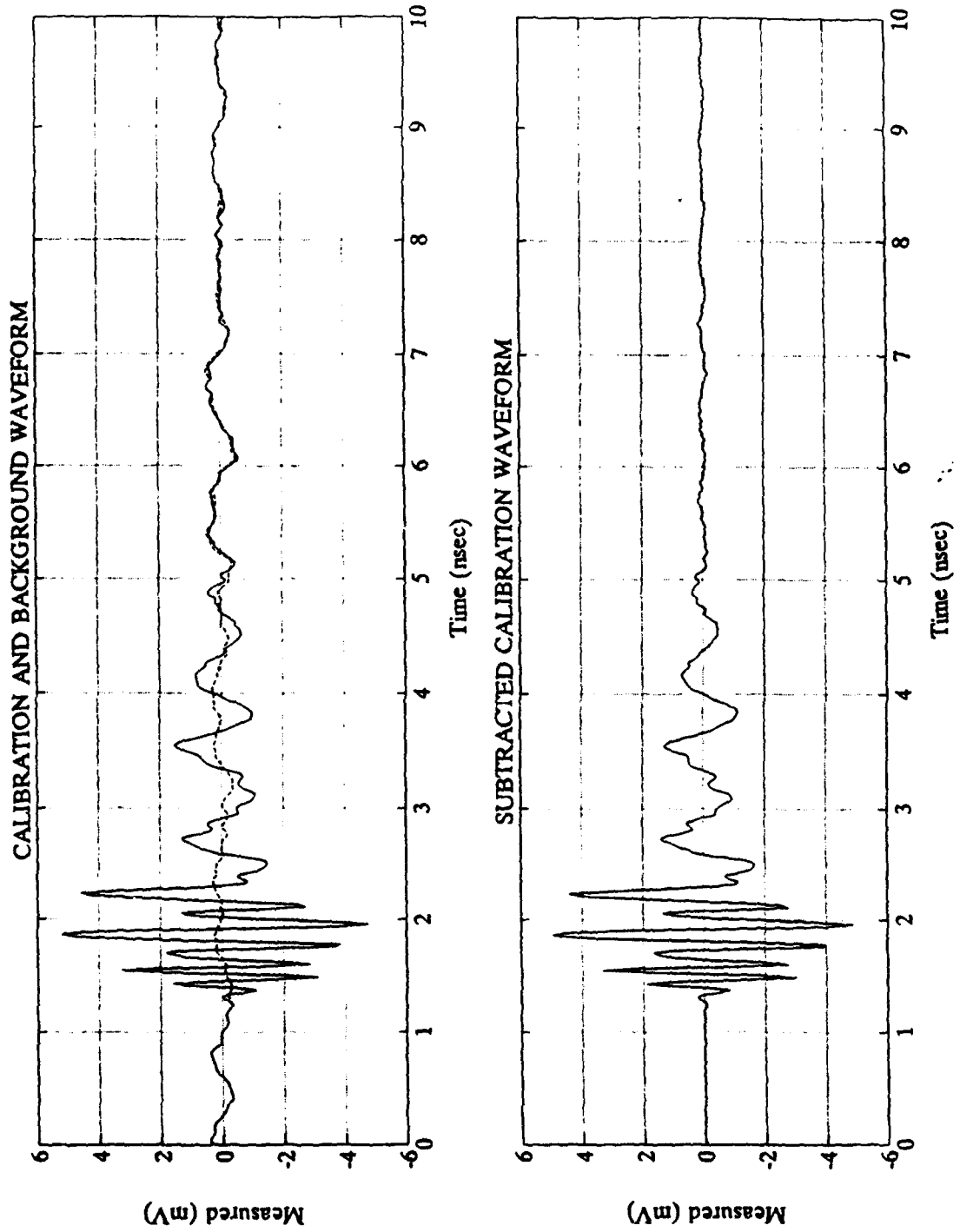


Figure 8. Calibration Measurement with 25.5 cm Delay Line

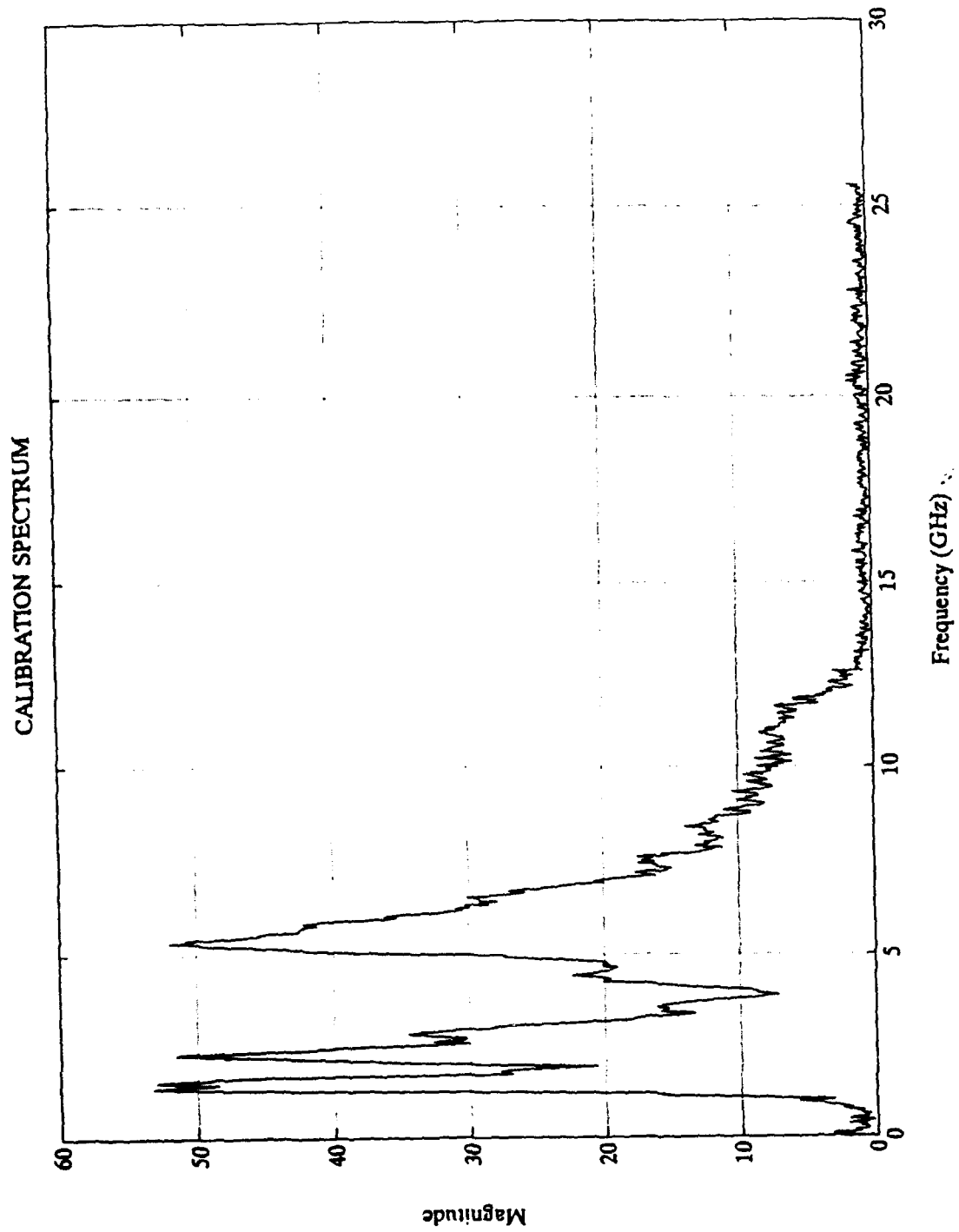


Figure 9. Calibration Spectrum with Minimum Delay Line

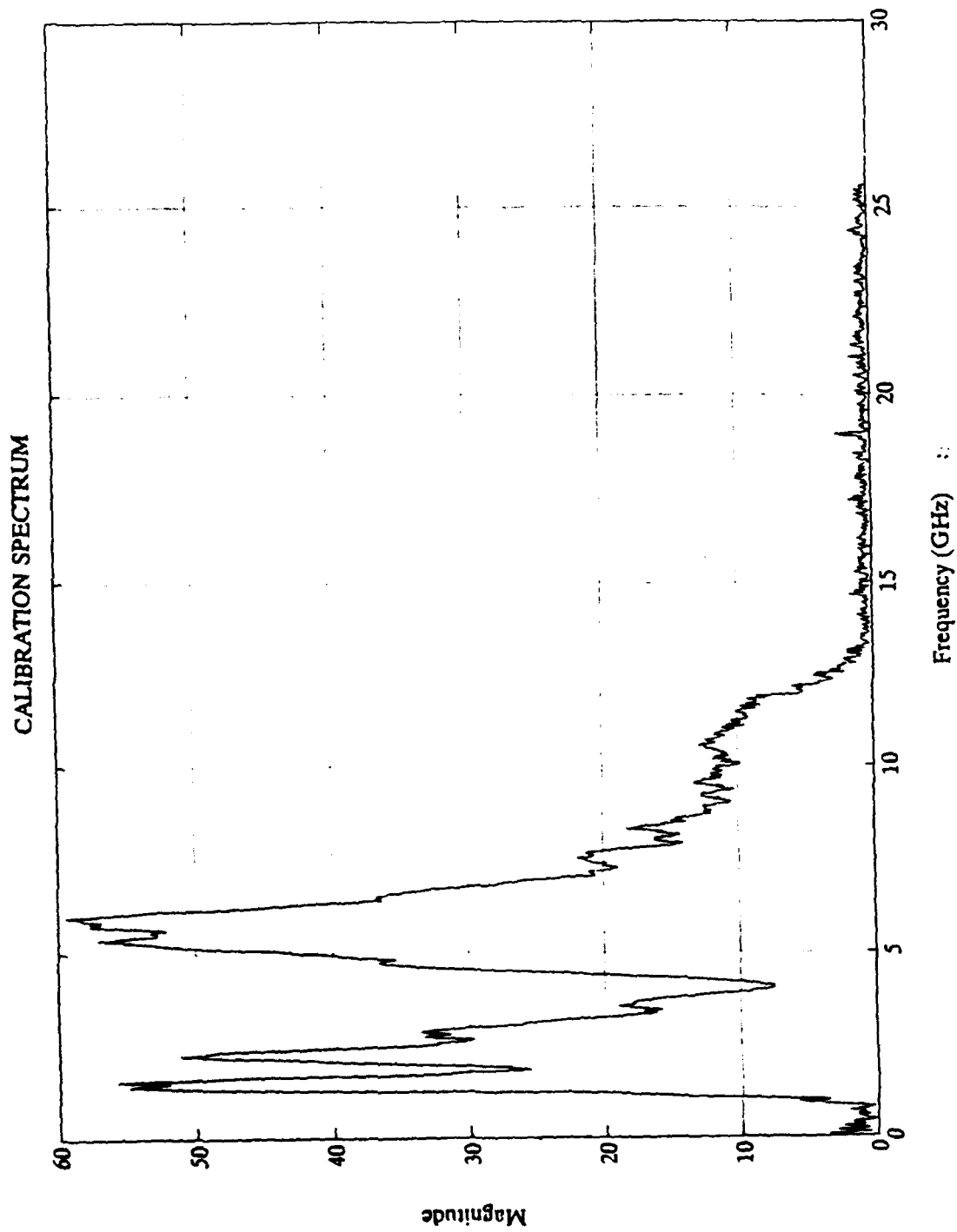


Figure 10. Calibration Spectrum with 25.5 cm Delay Line

The program then asks for the filename of the measured target waveform and the user has the option to use the same background waveform used for the calibration sphere or another background waveform. The program presents the same information and plots that were presented for the calibration sphere. Figures 11 to 14 show the 4" thin wire 90 degrees aspect measurement and the target spectrum for two different delay lines. After this, the program asks for the filename of the theoretically computed calibration sphere, which has already been calculated by the MIE and TSCT program as it was explained in Chapter III Section C, and plots the scattered response and its spectrum, as shown in Figure 15.

The next step requests entry of the smoothing parameter "C". The best results in this work were found by using "C" = 0.1. At this point the program has already computed the Fast Fourier Transform (FFT) of the subtracted calibration waveform, the subtracted target waveform and the computed calibration sphere. As a part of the optimal deconvolution estimator, the deconvolution component, which is given by equation 4.1, is formed and is shown in Figures 16 and 17 for two different delay lines.

$$Z(f) = \frac{Y_4^*(f) Y_5(f)}{Y_4(f) Y_4^*(f) + C} \quad (4.1)$$

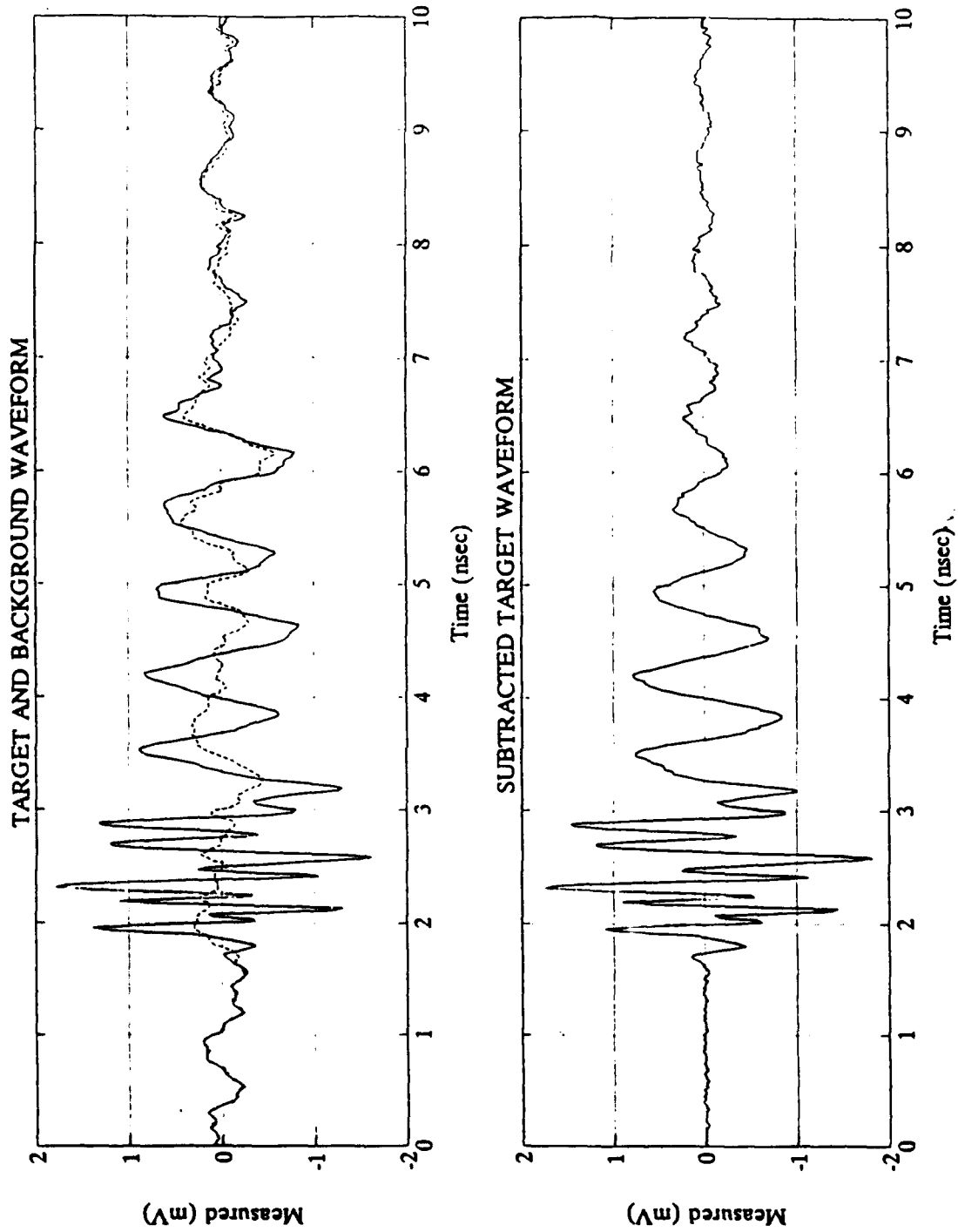


Figure 11. 4" Thin Wire Broadside Measurement with Minimum
 Delay Line (13.5cm)

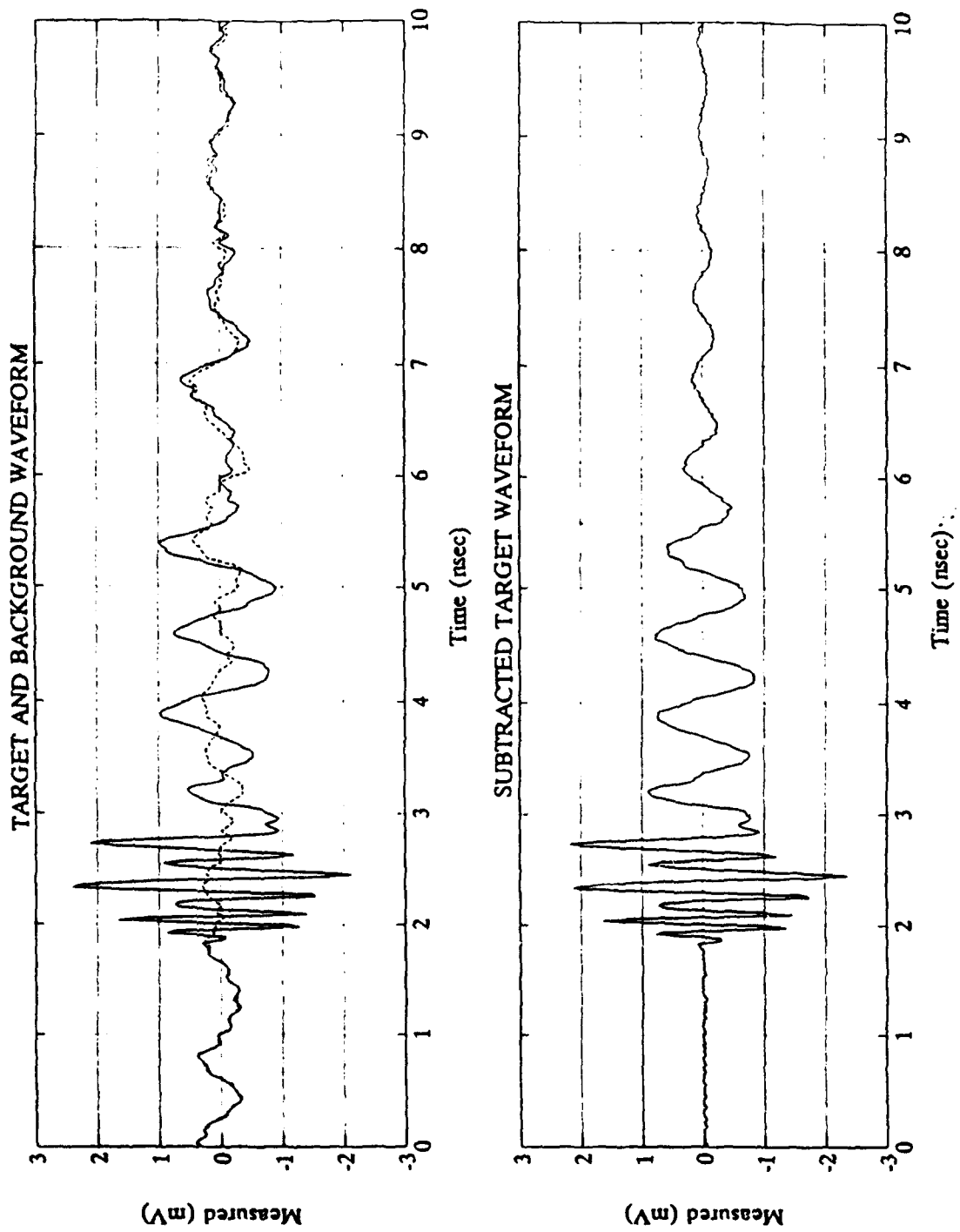


Figure 12. 4" Thin Wire Broadside Measurement with 25.5 cm Delay Line

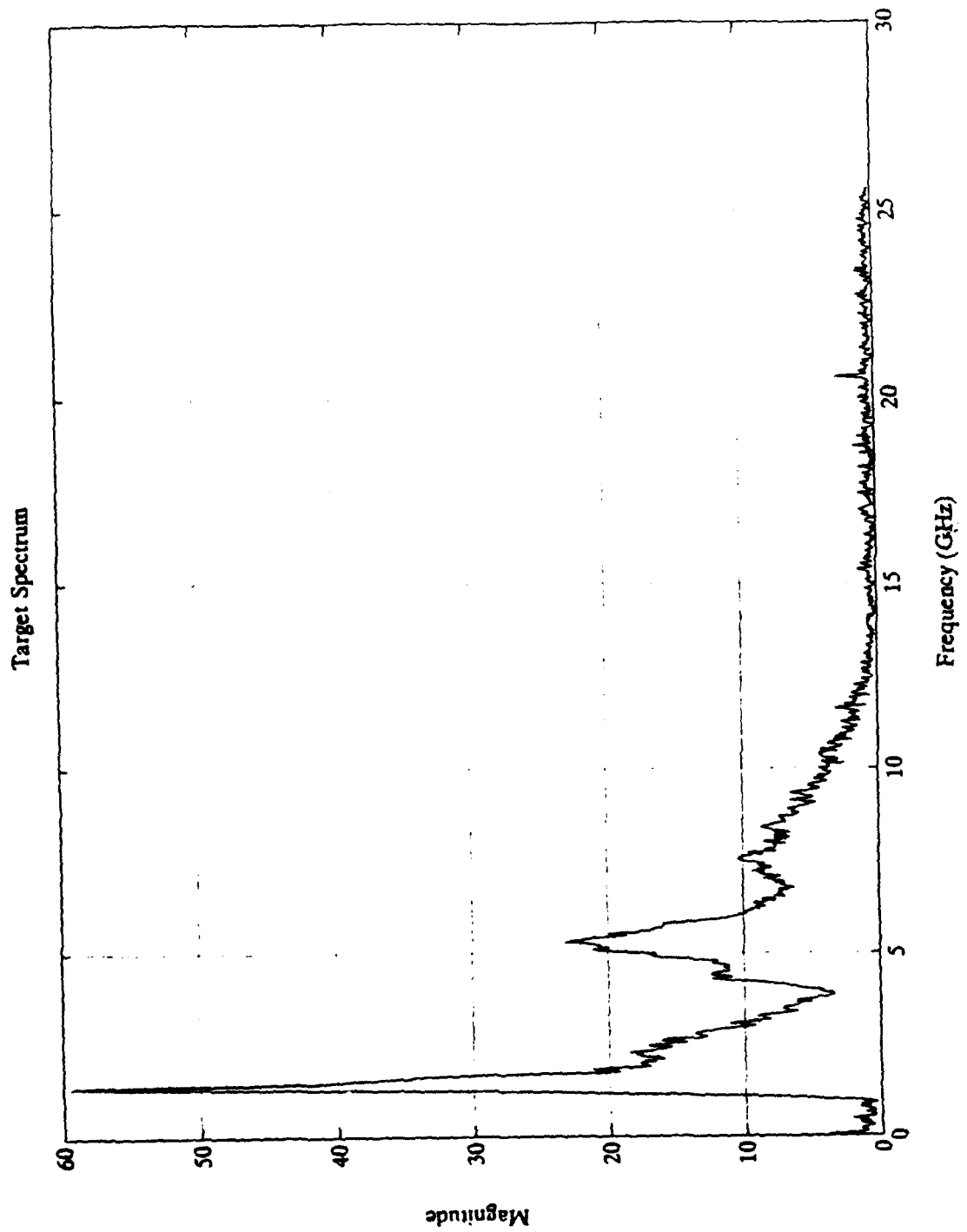


Figure 13. 4" Thin Wire Broadside Spectrum with Minimum Delay Line

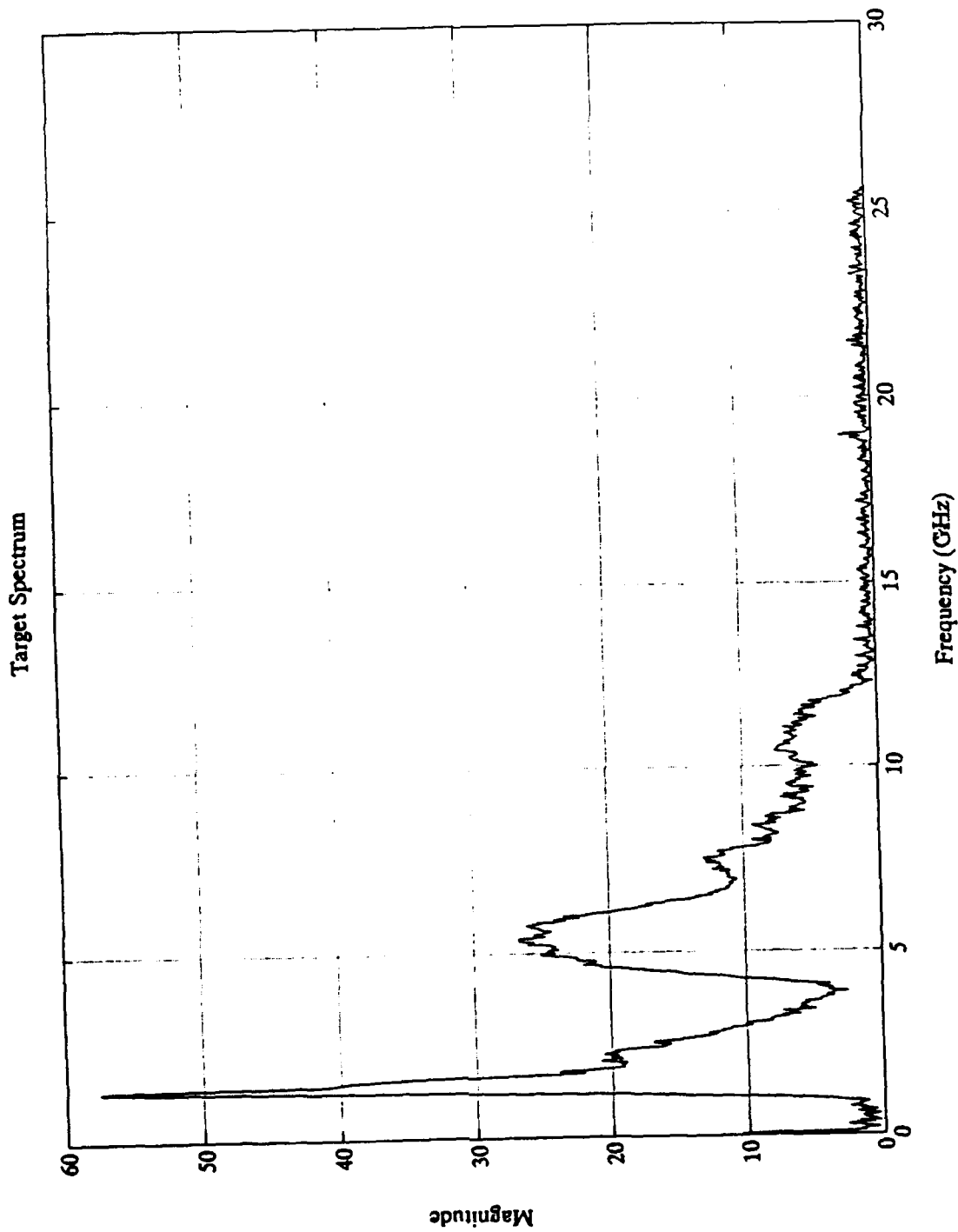


Figure 14. 4" Thin Wire Broadside Spectrum with 25.5 cm Delay
Line

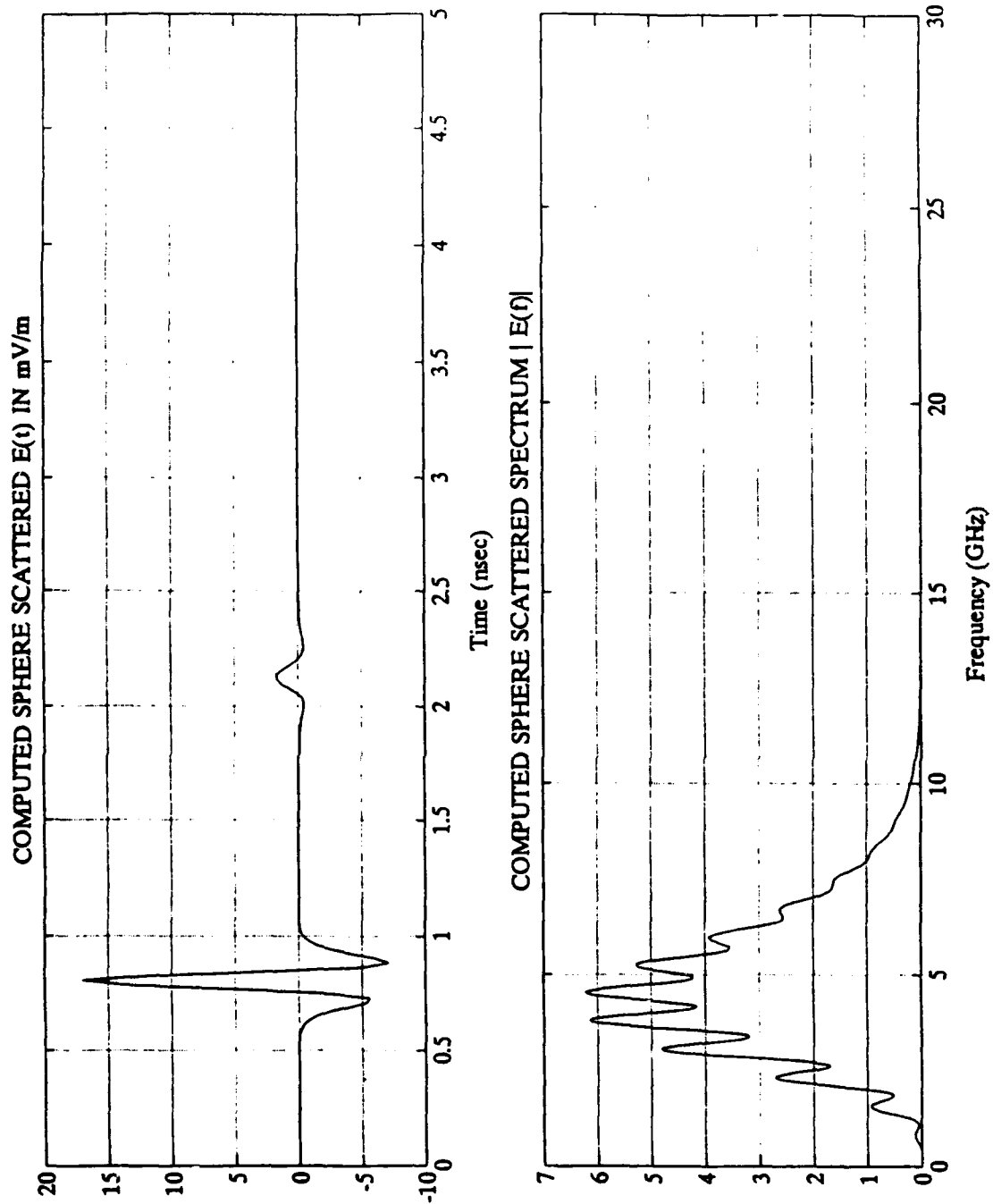


Figure 15. Time and Frequency Domain Plots for the Theoretically Computed Calibration Sphere

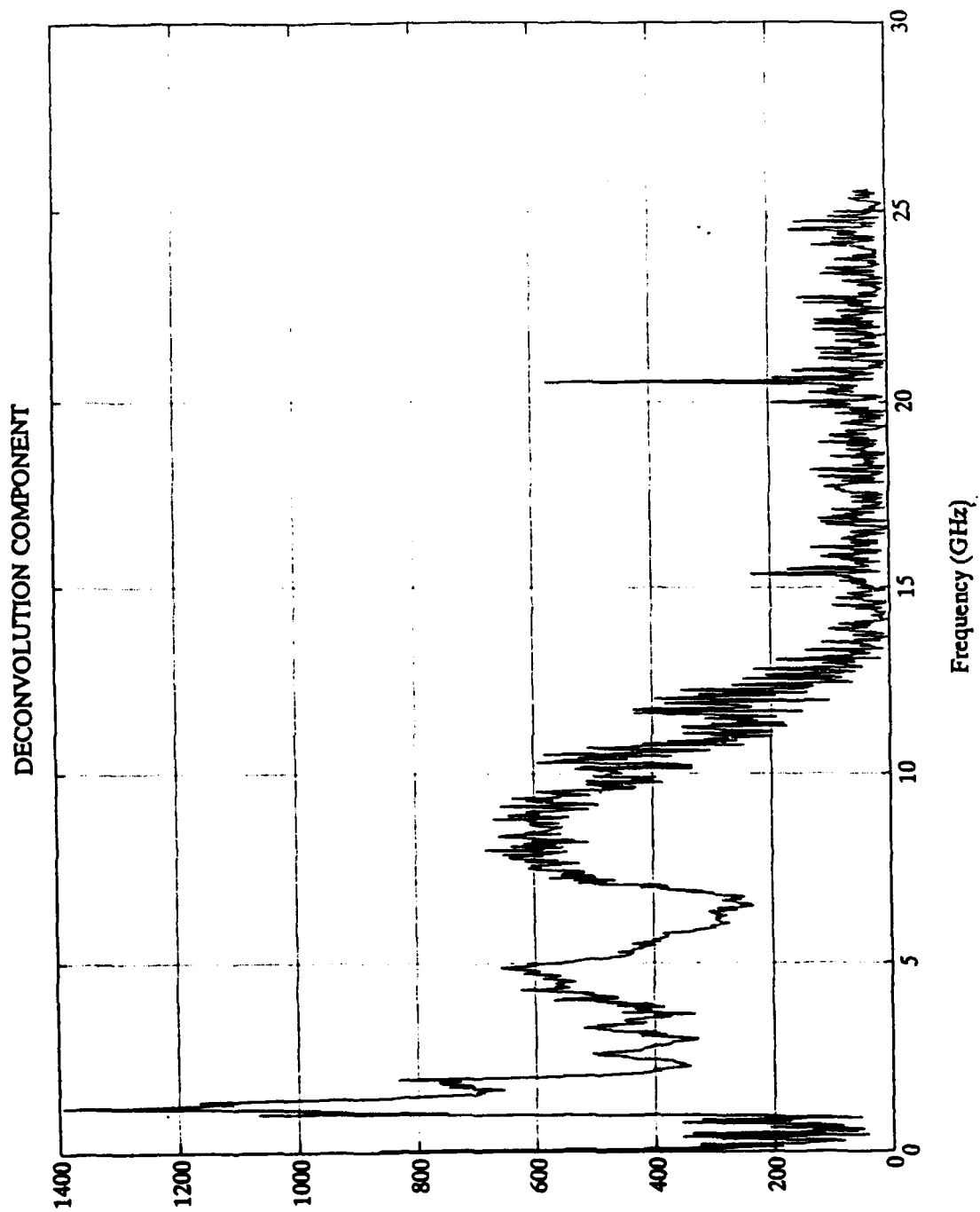


Figure 16. Deconvolution Component with Minimum Delay Line

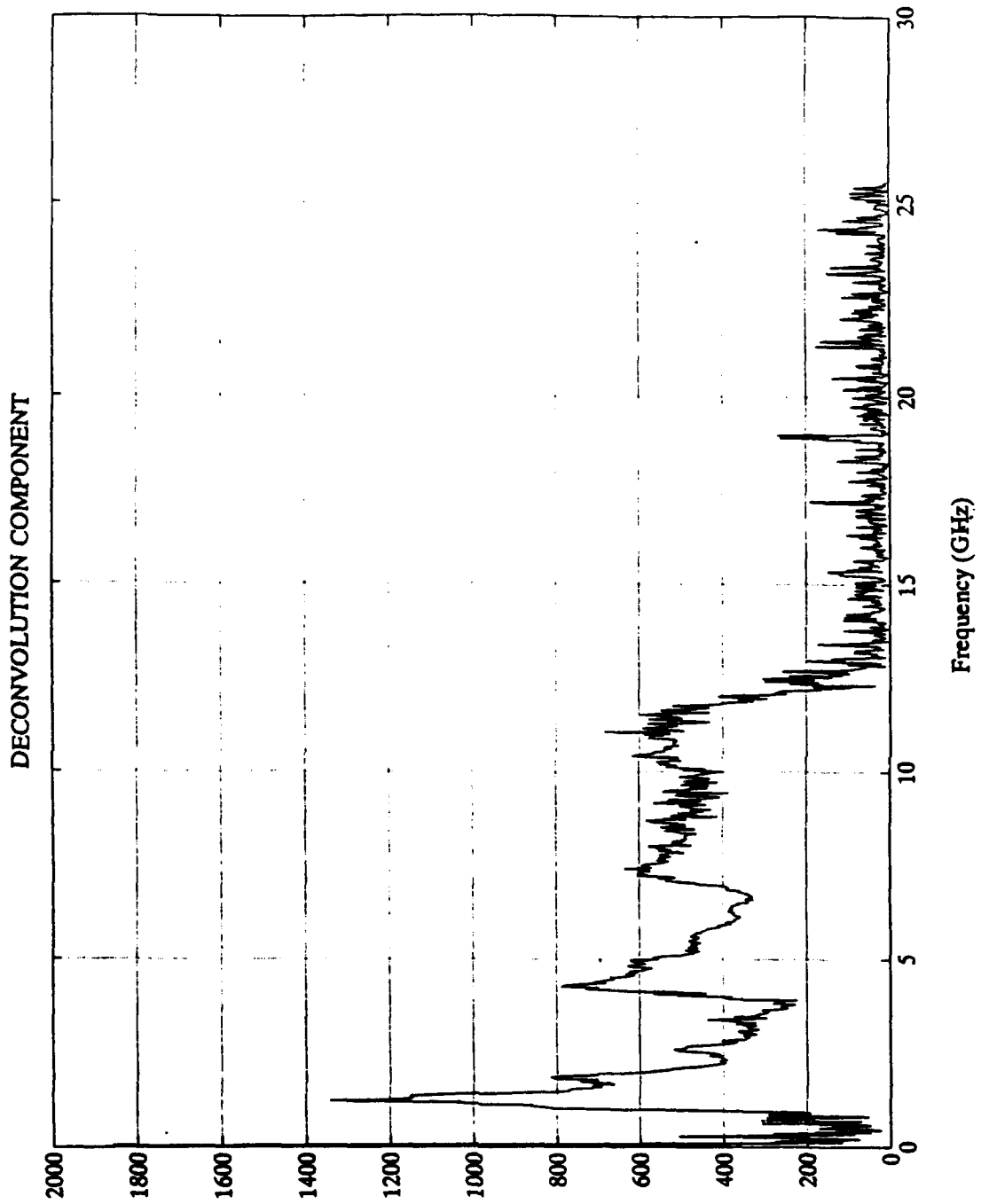


Figure 17. Deconvolution Component with 25.5 cm Delay Line

The deconvolution component is then multiplied by the FFT of the computed calibration sphere to complete the Riad's optimal deconvolution estimator. The deconvolution spectrum is then formed, as shown in Figures 18 and 19, for the 4" thin wire (broadside) and for two different delay lines. After this step the program takes the inverse FFT and plots the deconvolved field. Figures 20 and 21 show the deconvolved field for the 4" thin wire (broadside) for the two different delay lines. The program contains a "meta" file instruction which saves all the plots described in the process.

As previously explained in Chapter II Section B, the minimum coaxial line was set up in each amplifier. When the first set of measurements for the 4" thin wire were obtained and the data was processed by the deconvolution algorithm written in Fortran 77, an oscillation was noted at the front of the deconvolved field, as shown in Figure 20. When the deconvolution spectrum was compared with that obtained by Walsh [Ref. 5], no nulls were noted in the spectrum as were found in his work before he discovered the correct length for the delay line of the low frequency amplifier. For this reason, it was thought that there was not a phasing problem between the low and high frequency amplifiers. Several measurements were done for canonical targets and all the deconvolved fields showed the same undesired oscillation.

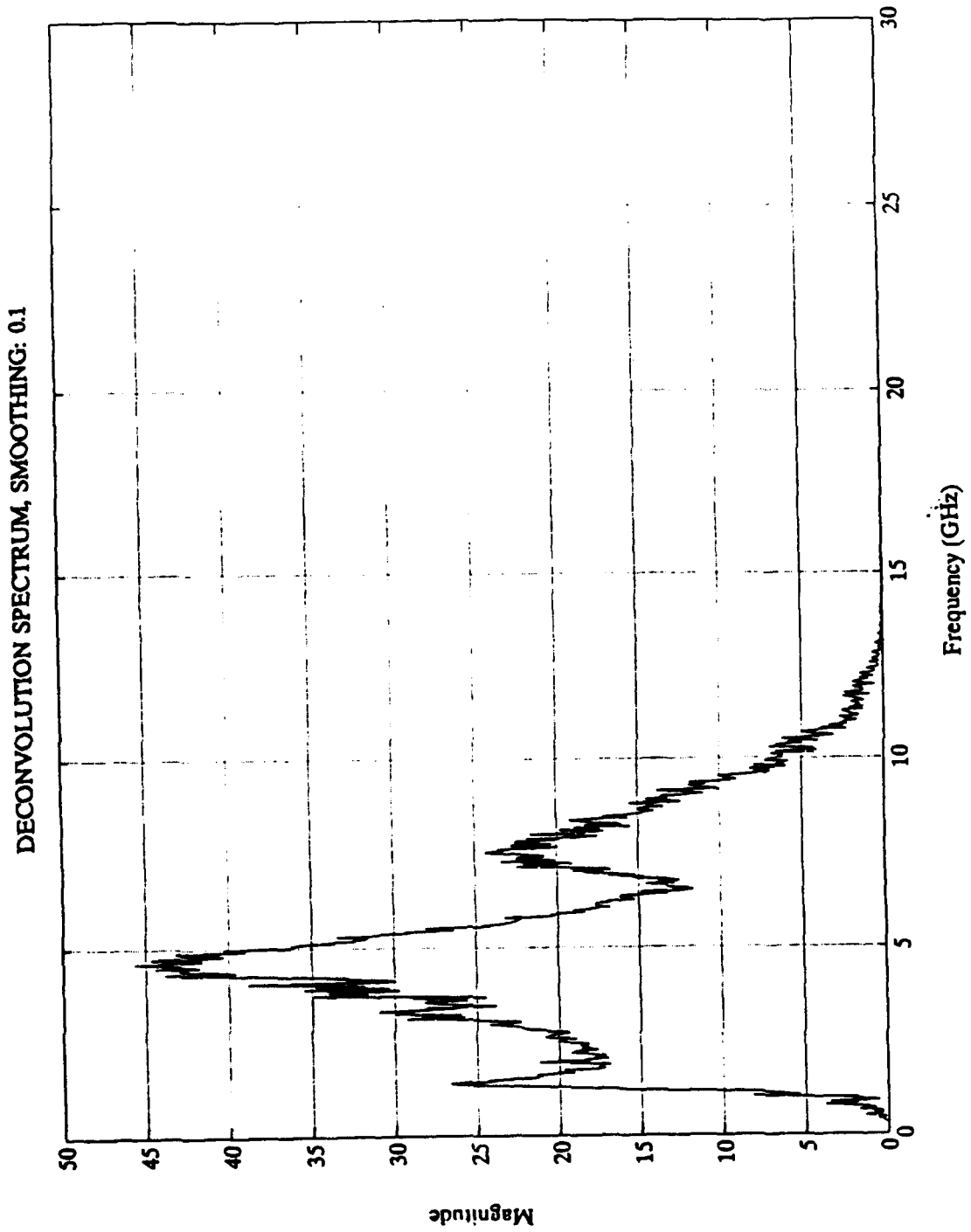


Figure 18. 4" Thin Wire Broadside Deconvolution Spectrum with Minimum Delay Line

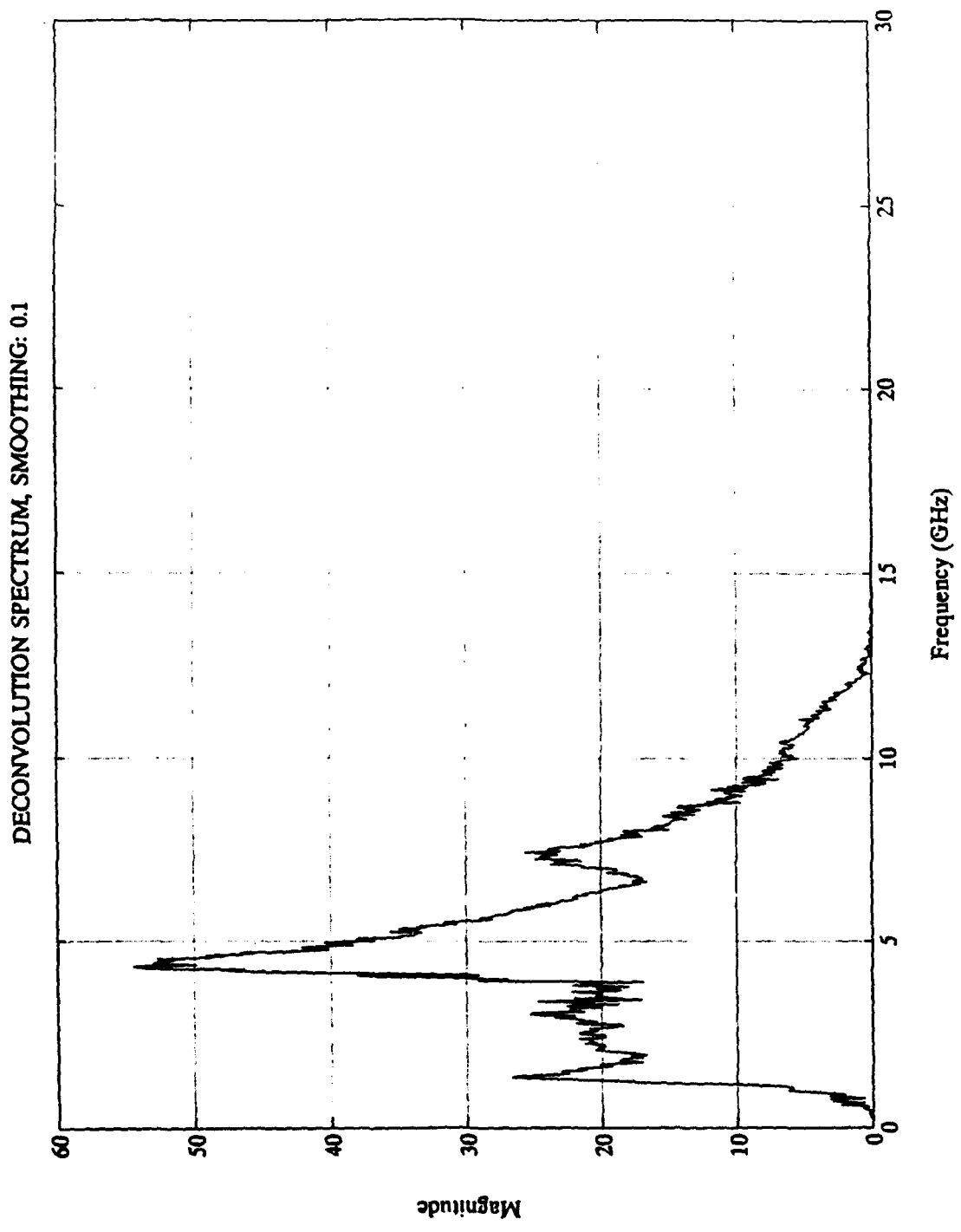


Figure 19. 4" Thin Wire Broadside Deconvolution Spectrum with
25.5 cm Delay Line

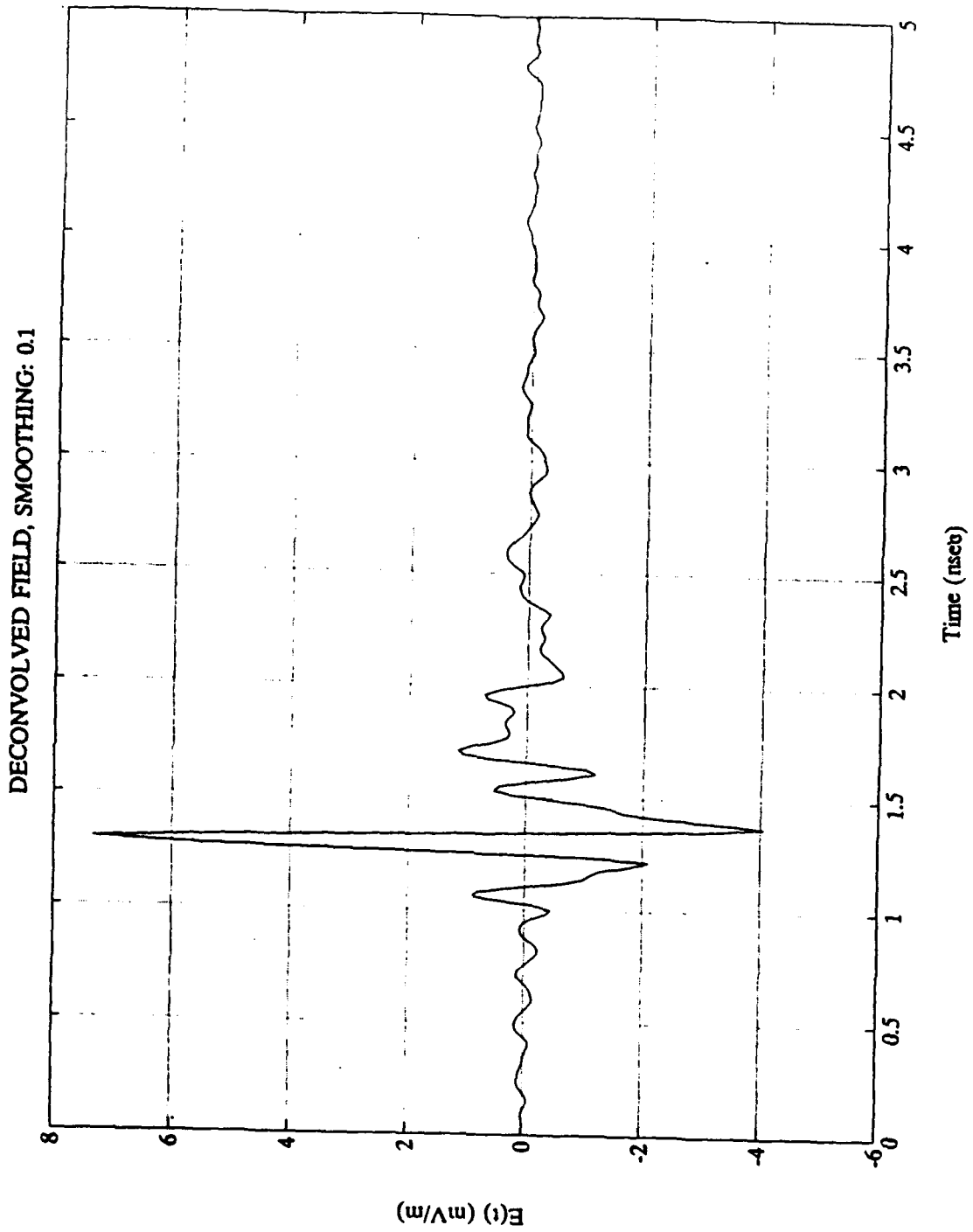


Figure 20. 4" Thin Wire Broadside Deconvolved Field with Minimum Delay Line

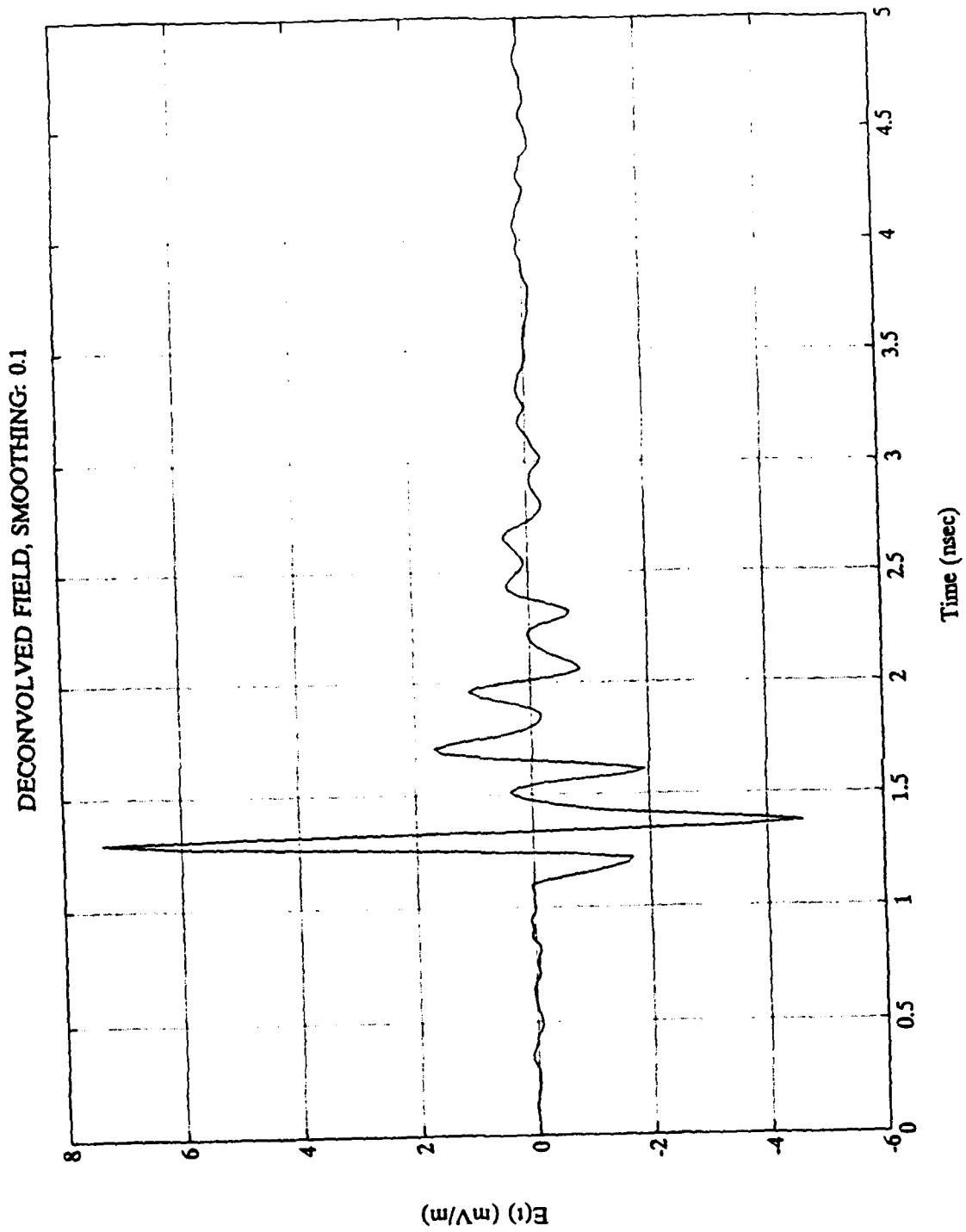


Figure 21. 4" Thin Wire Broadside Deconvolved Field with
25.5 cm Delay Line

The first attempt at elimination of the oscillation was directed towards reduction of the quantization of the DPO. Four measurements were required to do this. A calibration measurement with its respective background was performed using the DPO maximum vertical scale set to 16 mV and the 4" thin wire (broadside) with its background set to 8 mV maximum vertical scale. The same procedure was followed for other canonical targets like the 8 cm and 12 cm diameter spheres without improvement in the deconvolved fields.

The second trial was the modification of the deconvolution algorithm written in Fortran 77, to save the subtracted calibration and target waveforms. These files were then edited and the subtracted waveforms modified. The points before and after the response were zero padded. When the modified data were processed the deconvolved field still had the oscillation. The deconvolution algorithm was converted to Matlab and the same previous trials were performed with nearly identical results to those found using Fortran. A third trial modified the deconvolution component shown in Figures 16 and 17. The d.c. component, the frequency components up to 1 GHz and the frequency components from approximately 13 GHz to 25 GHz were made zero and it was multiplied by the FFT of the computed calibration sphere, to obtain the deconvolution spectrum. When the inverse FFT was taken to obtain the deconvolved field, no improvement was noted. The fourth trial included the measurements taken with an extra piece of a low

density styrofoam pedestal shown in Figure 1, because it looked like the targets were not perfectly aligned with the center of the antennas panel. Again, no improvement was obtained when the measurements were processed.

Next, the deconvolution algorithm written in Matlab was modified and called Time Domain Deconvolution. This is explained in more detail in the next subsection. Equation 4.1, which represents the deconvolution component in the frequency domain, was transformed to the time domain and the deconvolved impulse response was formed. This impulse response was convolved with the time domain computed calibration sphere to form the hybrid deconvolved field. The same undesired response was observed.

During another test the deconvolved impulse response waveform shown in Figure 24 was modified. The points before the impulse response were made zero. When this modified waveform was convolved with the time domain computed calibration sphere, the oscillation at the front of the hybrid deconvolved field disappeared. It was thought that the oscillation could be caused by a d.c. component present in the measurements. A new set of complete measurements were done with a d.c. blocking capacitor installed at the output of the receiving antenna. After the signal processing the oscillation still existed.

A new program in Matlab was created to verify the effect of the delay line in both amplifiers. A set of three

measurements required by the process were obtained with just the low frequency amplifier while the other amplifier was replaced by a dummy load. The same procedure was followed for the high frequency amplifier. The program begins by asking the user how many time points to shift the low frequency signal. The program then asks for the filenames of each of the six waveforms and forms four subtracted waveforms as it was explained for the deconvolution algorithm. Once this has been done the program adds the corresponding subtracted waveforms for both amplifiers and follows the procedure described before. It was determined, in case of the values shown in Chapter II Section B, that each time point is equivalent to approximately 4 mm of delay line. Several trials were performed, sweeping from 1 to 100 time points for the low frequency signals. It was noted that the delay line had a large effect in the final deconvolved field. The same procedure was performed to shift the high frequency signals. The user must keep in mind that the program has been designed to shift just the low frequency signals, so in order to shift the high frequency signals, the user must input the data filename of the 6-12 GHz when the program requests the data filenames for the 1-6 GHz and vice versa.

The best result was obtained by shifting the signal of the low frequency amplifier by 30 time points. These 30 time points are equivalent to an extra delay of 12 cm, as shown in Chapter II Section B. These measurements were done with a

minimum delay line for both amplifiers. With this result, a 25.5 cm delay line was constructed for the low frequency amplifier, thus giving 13.5 cm corresponding to the minimum delay and 12 cm corresponding to the extra delay. When the measurements were done with the new delay the undesired oscillation was not present, as is shown in Figures 21 and 27. Several sets of measurements for canonical targets were done with this new delay line yielding excellent results that agree with the theoretical waveforms, as will be shown in the next section.

It can be clearly observed in Figures 7 and 11, in comparison with Figures 8 and 12 presented in this subsection, that with the minimum delay line the low frequency bandpass signal was arriving at the DPO sampling head before the high frequency component. After the 25.5 cm delay line was installed, both signals are arriving at the DPO sampling head at the same time. The effect of the delay line in the final deconvolved field is critical to obtain desired waveforms, as shown in Figure 21. Conversely, if the delay line does not provide simultaneous signal arrival, an unacceptable waveform, which includes a series of additional oscillations, will occur. A simulation using a 35.5 cm delay line (55 time points) was introduced for the low frequency amplifier yielding Figure 22. This is a very undesirable waveform although its spectrum, Figure 23, does not display any deep nulls as presented by Walsh [Ref. 5].

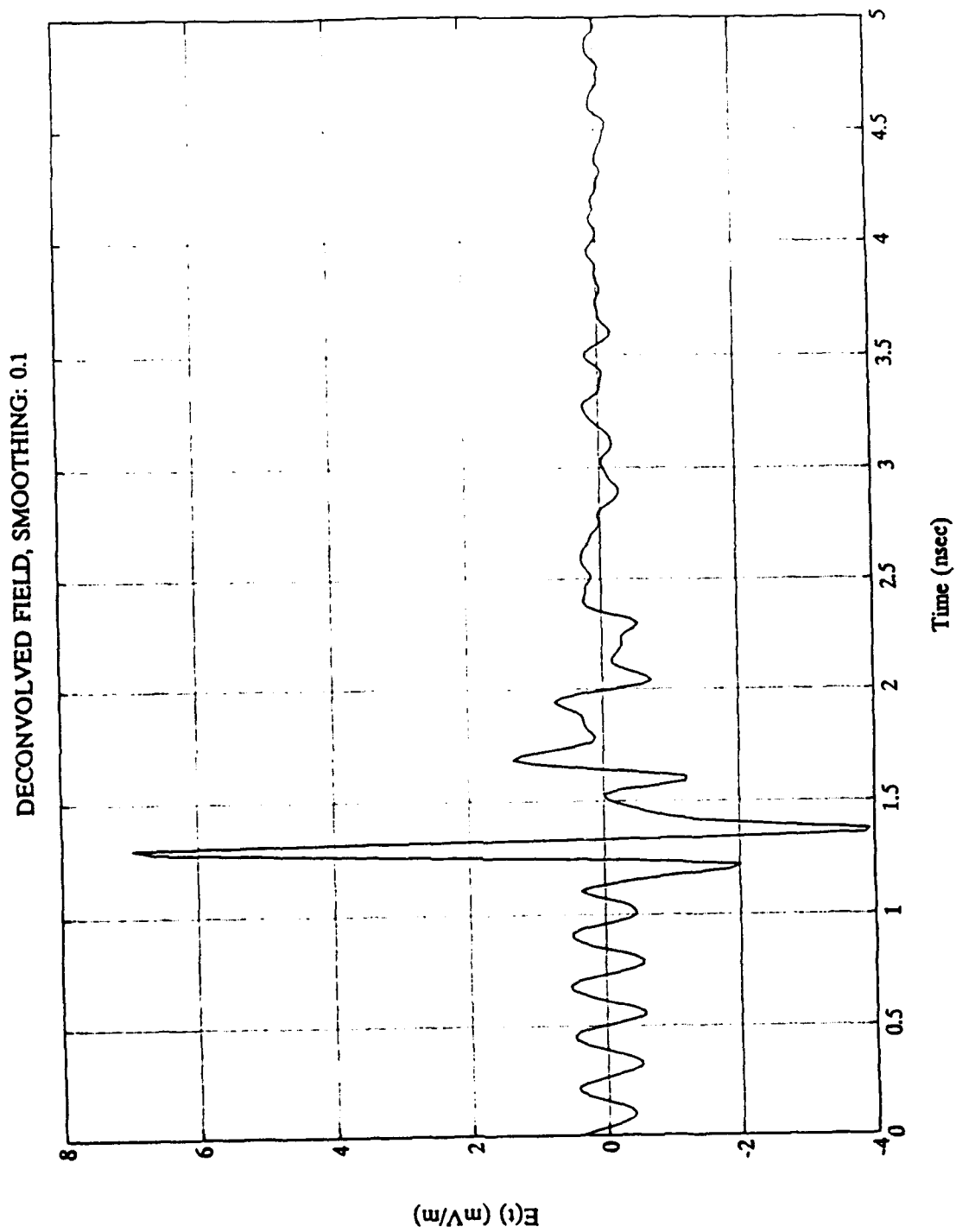


Figure 22. 4" Thin Wire Broadside Deconvolved Field with a
Simulated 35.5 cm Delay Line

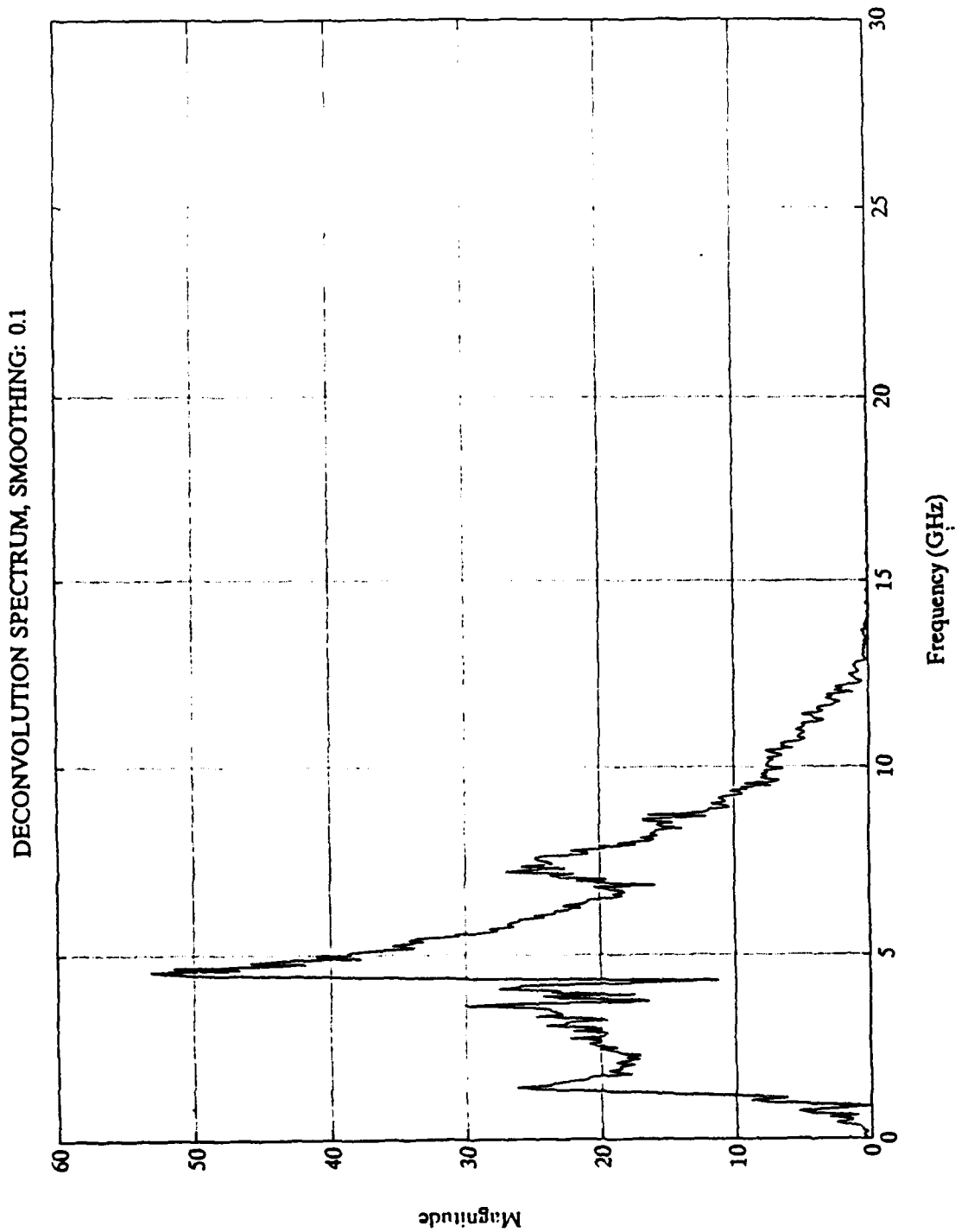


Figure 23. 4" Thin Wire Broadside Deconvolution Spectrum with
a Simulated 35.5 cm Delay Line

2. Time Domain Deconvolution

The time domain deconvolution algorithm (TDDA) is a continuation of the frequency domain deconvolution algorithm (FDDA). The optimal deconvolution estimator described in Chapter III can be evaluated completely in the time domain for the case of no smoothing (e.g. $C=0$).

Both the FDDA and TDDA were computed in the same program. The FDDA calculates the deconvolved field by multiplying the deconvolution component, presented in equation 4.1, with the FFT of the computed calibration sphere followed by an inverse FFT. Unlike the FDDA, the TDDA calculates the deconvolved field by taking the inverse FFT of the deconvolution component, forming the deconvolved impulse response, and convolving it with the computed calibration sphere as shown in equation 4.2.

$$x_0(t) h_{xs}(t) = \mathcal{F}^{-1} \left[\frac{Y_4^*(f) Y_5(f)}{Y_4(f) Y_4^*(f) + C} \right] \star [x_0(t) h_{ys}(t)] \quad (4.2)$$

The two components of the convolution specified by equation 4.2, the computed calibration sphere and the deconvolved impulse response, are shown in Figures 24 and 25 for a 4" thin wire (broadside) and for two different delay lines. The hybrid deconvolved fields are shown in Figures 26 and 27. Figure 27 displays excellent agreement with its respective theoretical one.

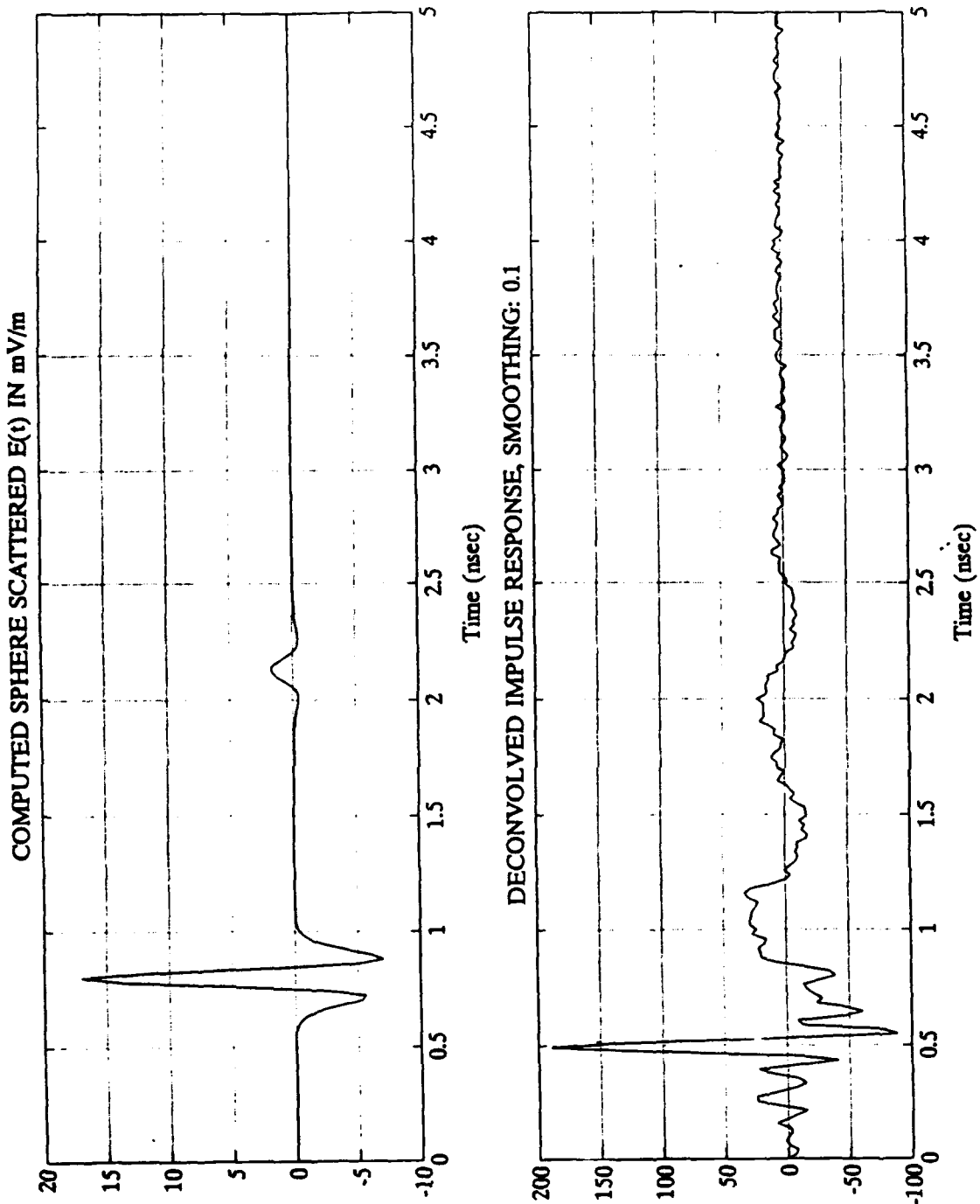


Figure 24. Computed Calibration Sphere and 4" Thin Wire
 Broadside Deconvolved Impulse Response with Minimum Delay Line

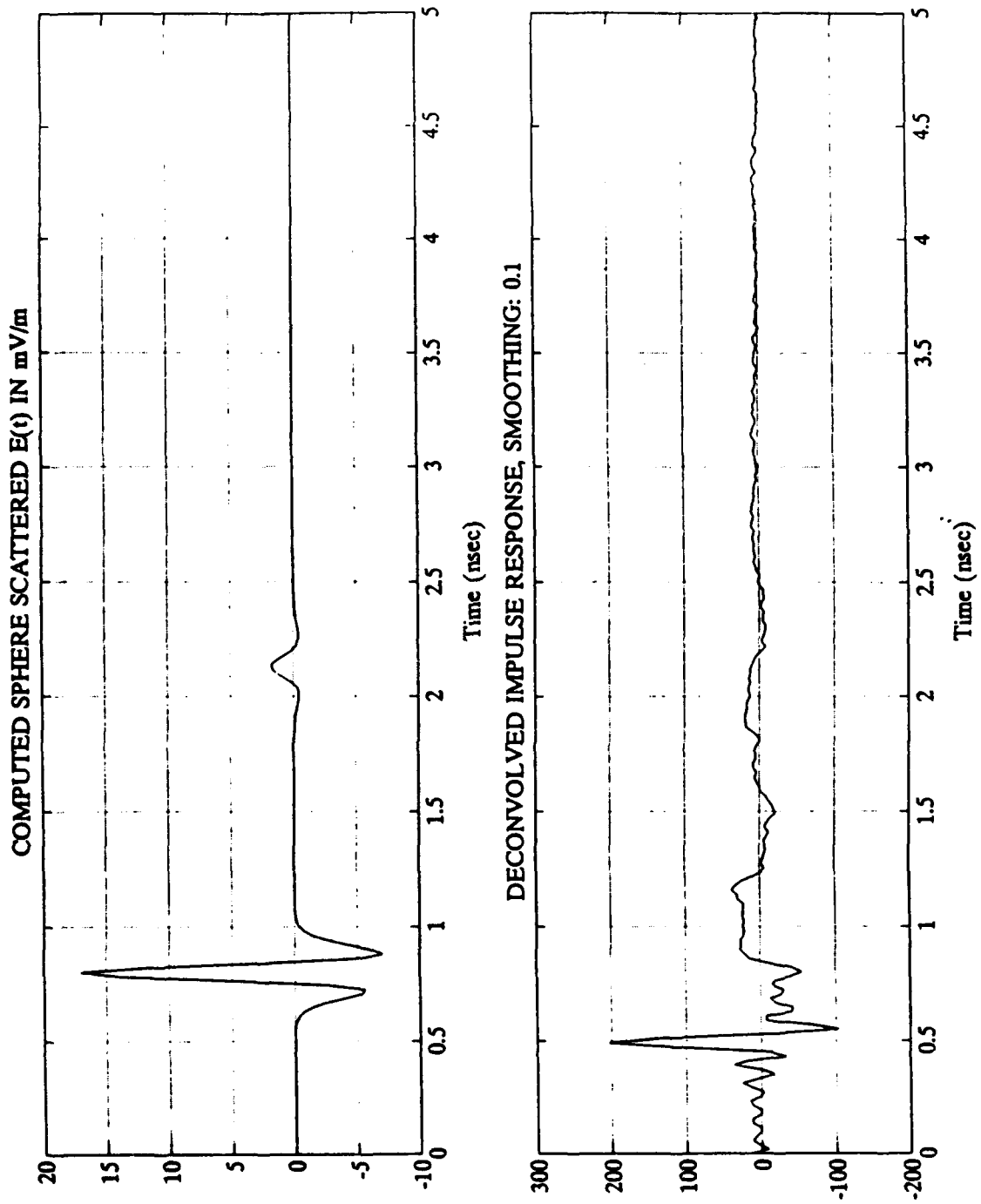


Figure 25. Computed Calibration Sphere and 4" Thin Wire
 Broadside Deconvolved Impulse Response with 25.5 cm Delay Line

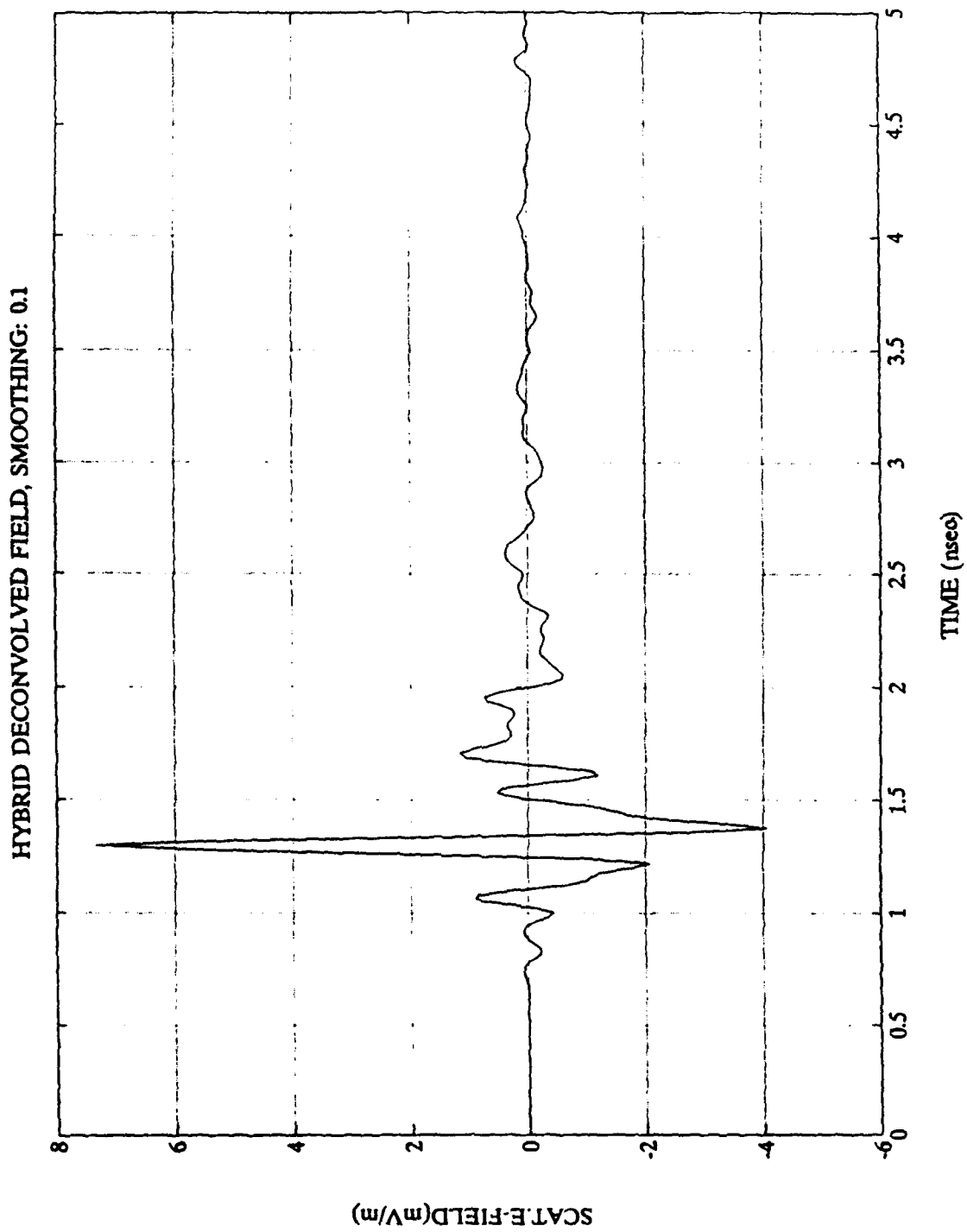


Figure 26. 4" Thin Wire Broadside Hybrid Deconvolved Field
with Minimum Delay Line

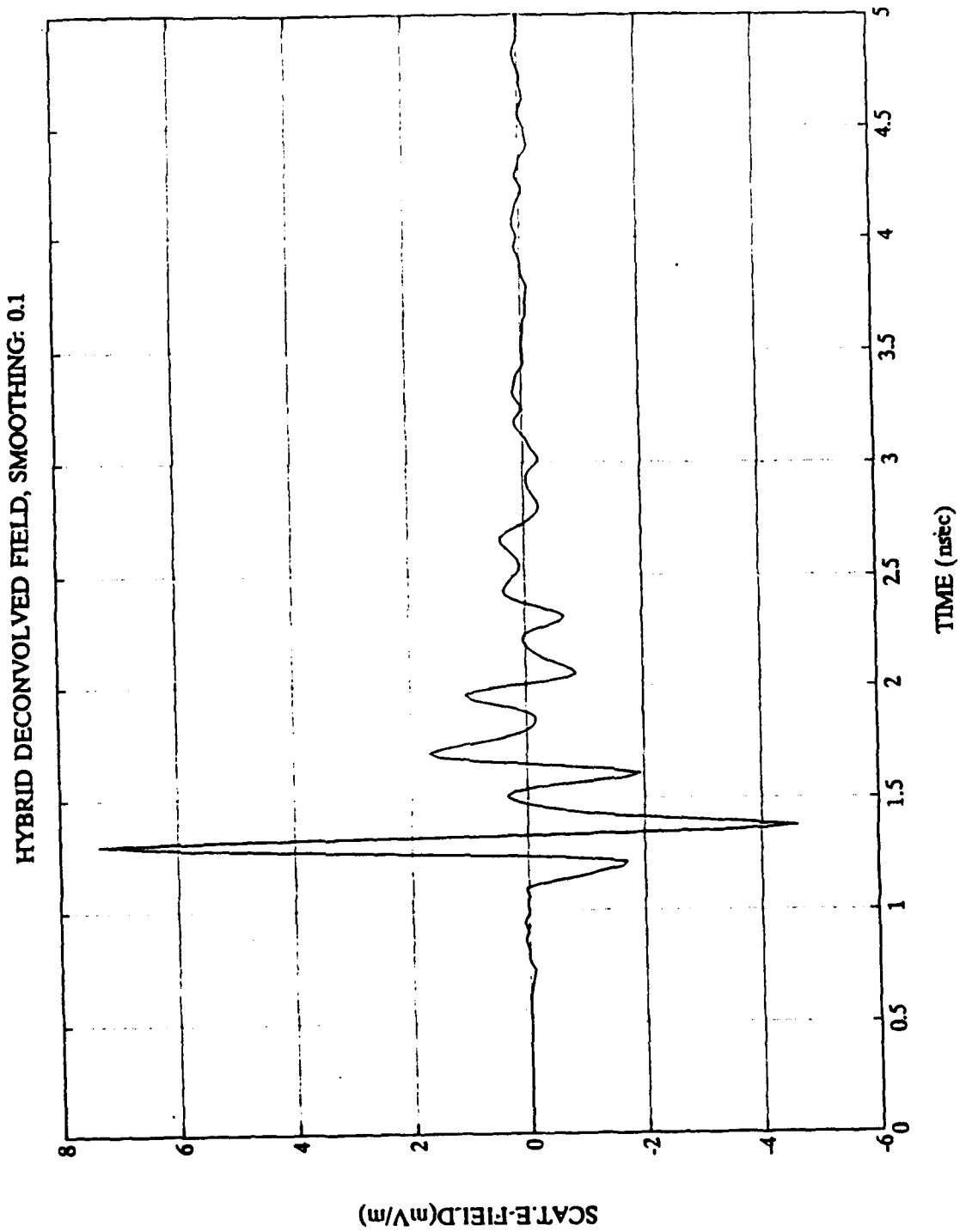


Figure 27. 4" Thin Wire Broadside Hybrid Deconvolved Field
with 25.5 cm Delay Line

C. SYSTEM VALIDATION

Validation of the upgraded Transient Electromagnetic Scattering Laboratory was performed by comparing experimentally obtained deconvolved fields with theoretically computed waveforms for canonical targets. These canonical targets are:

- 1) 8 centimeter diameter metal sphere.
- 2) 12 centimeter diameter metal sphere.
- 3) 10 cm long, 2.36 millimeter diameter thin wire 90 degrees aspect (broadside).
- 4) 10 cm long, 2.36 millimeter diameter thin wire 30 degrees aspect.

The theoretical responses for the 8 cm and 12 cm spheres are obtained by the two programs, MIE and TSCT, as mentioned in Chapter III. MIE calculates the magnitude and phase of the sphere's transfer function. The inputs used in this program are summarized in Table 2. TSCT takes the files created by MIE and computes the scattering response due to an incident double Gaussian pulse. Table 3 summarizes the inputs used in the TSCT program.

Another program written by M.A. Morgan, called TDIE-DG, computes the theoretical scattering response for the thin wire due to a double Gaussian pulse. The program makes the discretization and solves a time domain integral equation to calculate the induced currents in time and space. The program then computes the backscattering far field, using the

currents, by a numerical time space integration. The user supplied inputs used in TDIE-DG are summarized in Table 4.

TABLE 2. NUMERICAL COMPUTATIONS INPUTS OF MIE PROGRAM

Enter filename of magnitude and phase array	Selected by the user
Number of frequency segments	512
Sphere radius in meters	0.04, 0.06
Distance from sphere in meters	2.18
Bistatic angle in degrees	4.5
Scattering plane	E plane
Time window in nsec	20

TABLE 3. NUMERICAL COMPUTATIONS INPUTS OF TSCT PROGRAM

Enter data filename for magnitude and phase created by MIE	As selected by the user in MIE
Narrow 10% PW in nsec	0.15
Wide 10% PW in nsec	0.30
Extra time delay in nsec	1

TABLE 4. NUMERICAL COMPUTATIONS INPUTS OF TDIE-DG PROGRAM

Wire length in meters	0.1
Number of wire segments	17
Wire radius in meters	0.00117
Incident Alpha angle in degrees	30, 90
Time window in nsec	20
Filename for I(t,z) storage	Selected by the user
Narrow 10% PW in nsec	0.15
Wide 10% PW in nsec	0.30
Time delay in nsec	1
Far field computation	Yes
Distance in meters	2.18
Theta in degrees for far field computation = 180 - Alpha	150, 90

Figures 28, 29, 30, and 31 compare the theoretical and deconvolved waveforms for the canonical targets described in this section. The high level of accuracy obtained by the new TESL configuration and the algorithms used are apparent from these examples.

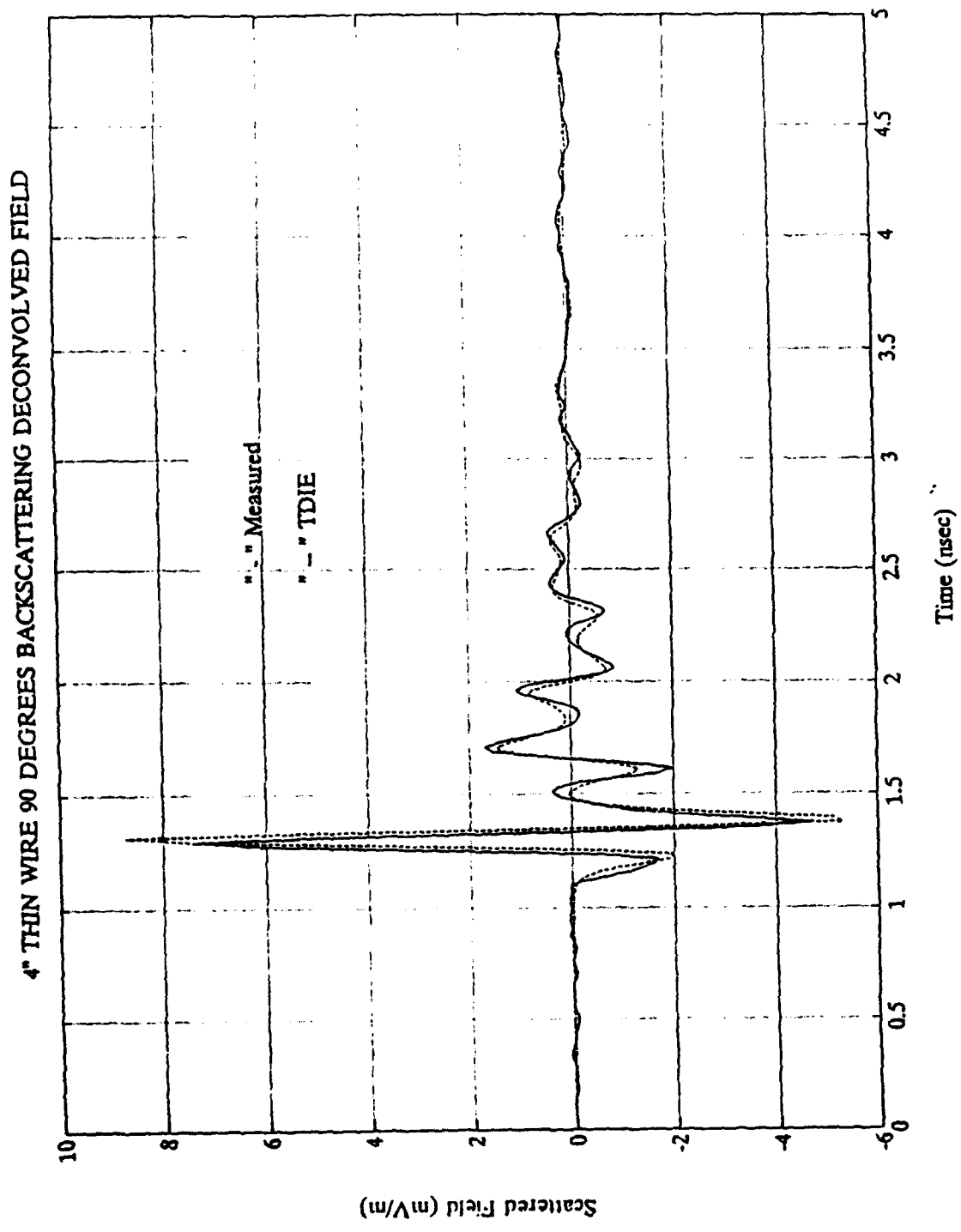


Figure 28. 4" Thin Wire Broadside Validation

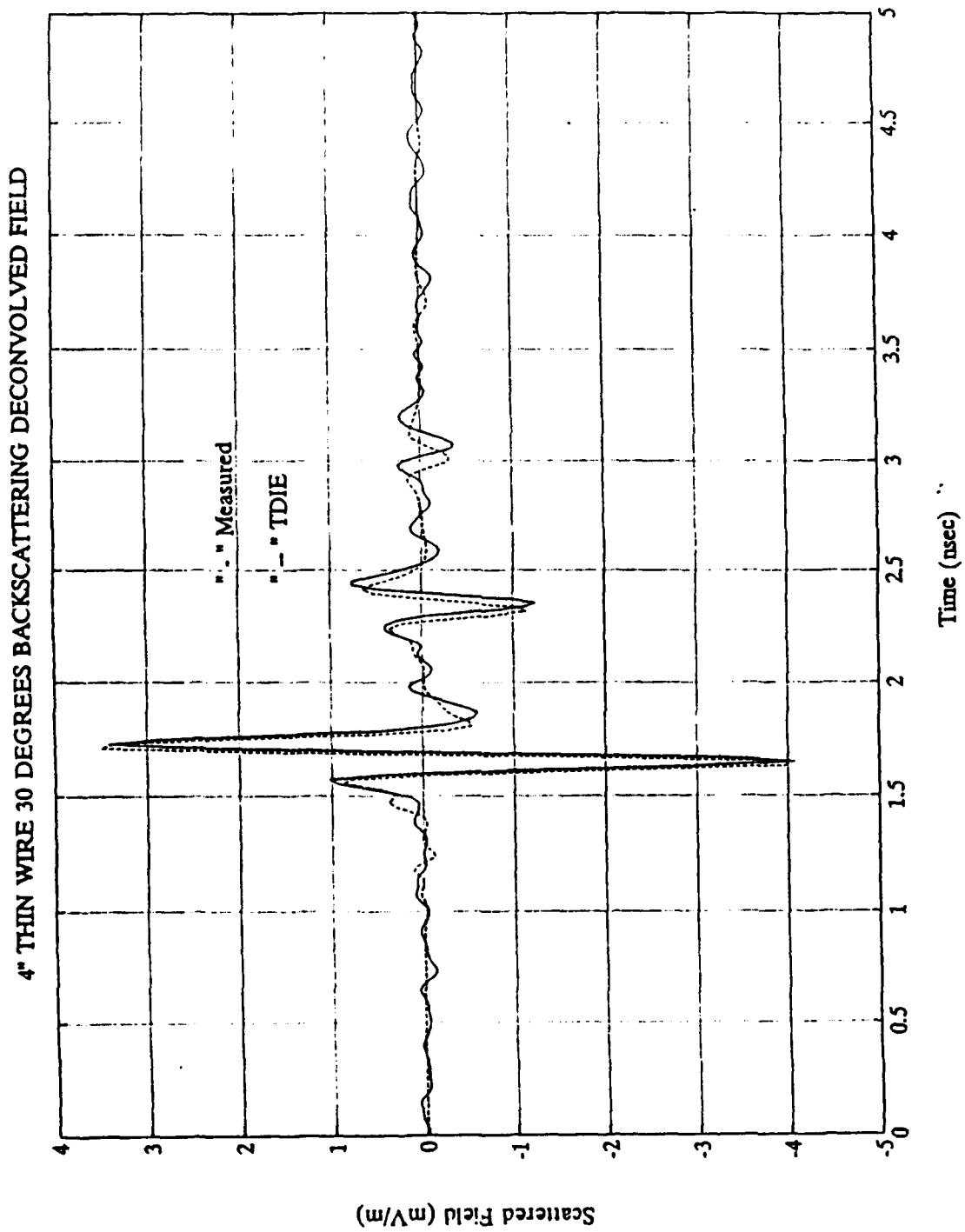


Figure 29. 4" Thin Wire 30 Degrees Aspect Validation

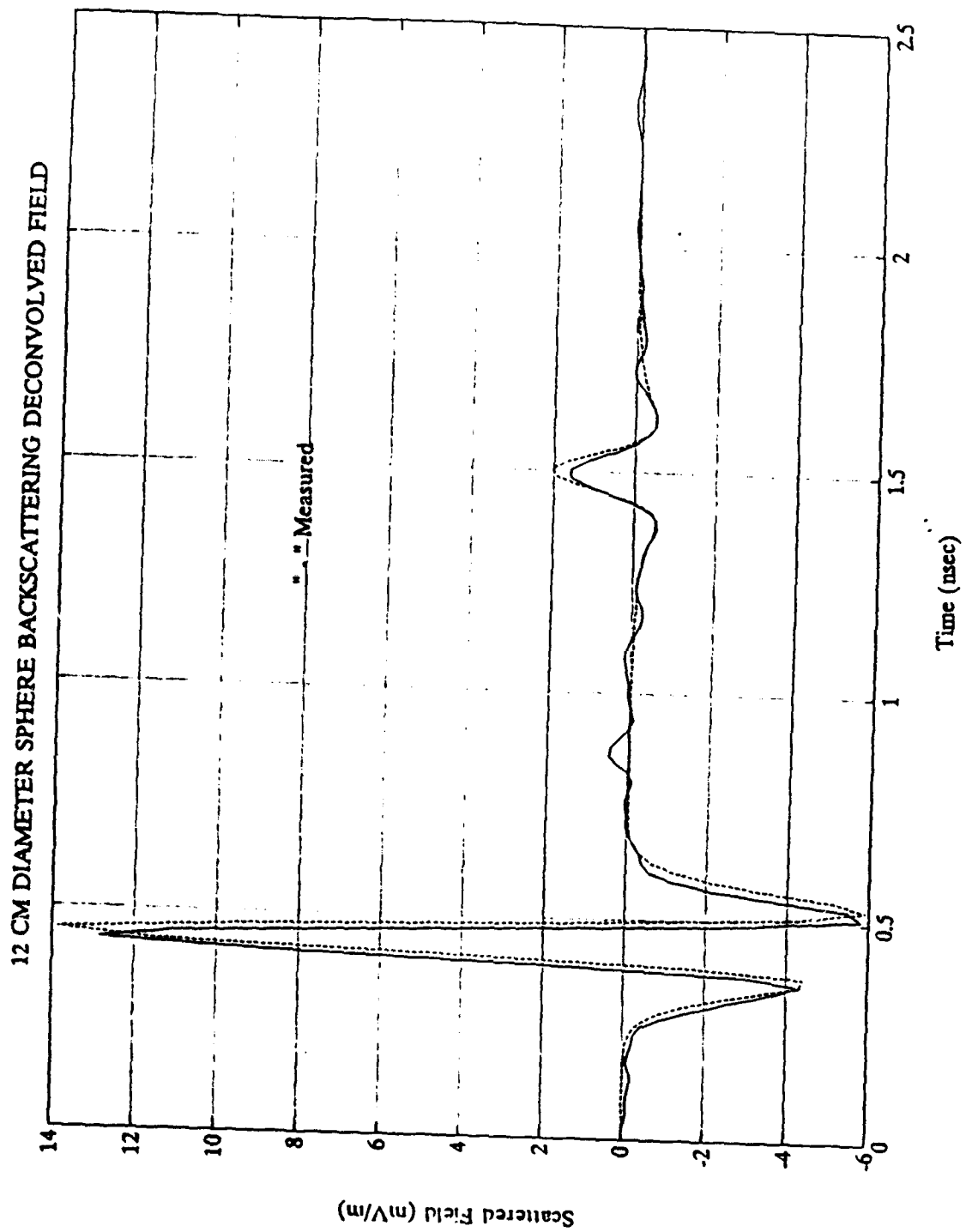


Figure 30. 12 cm Diameter Sphere Validation

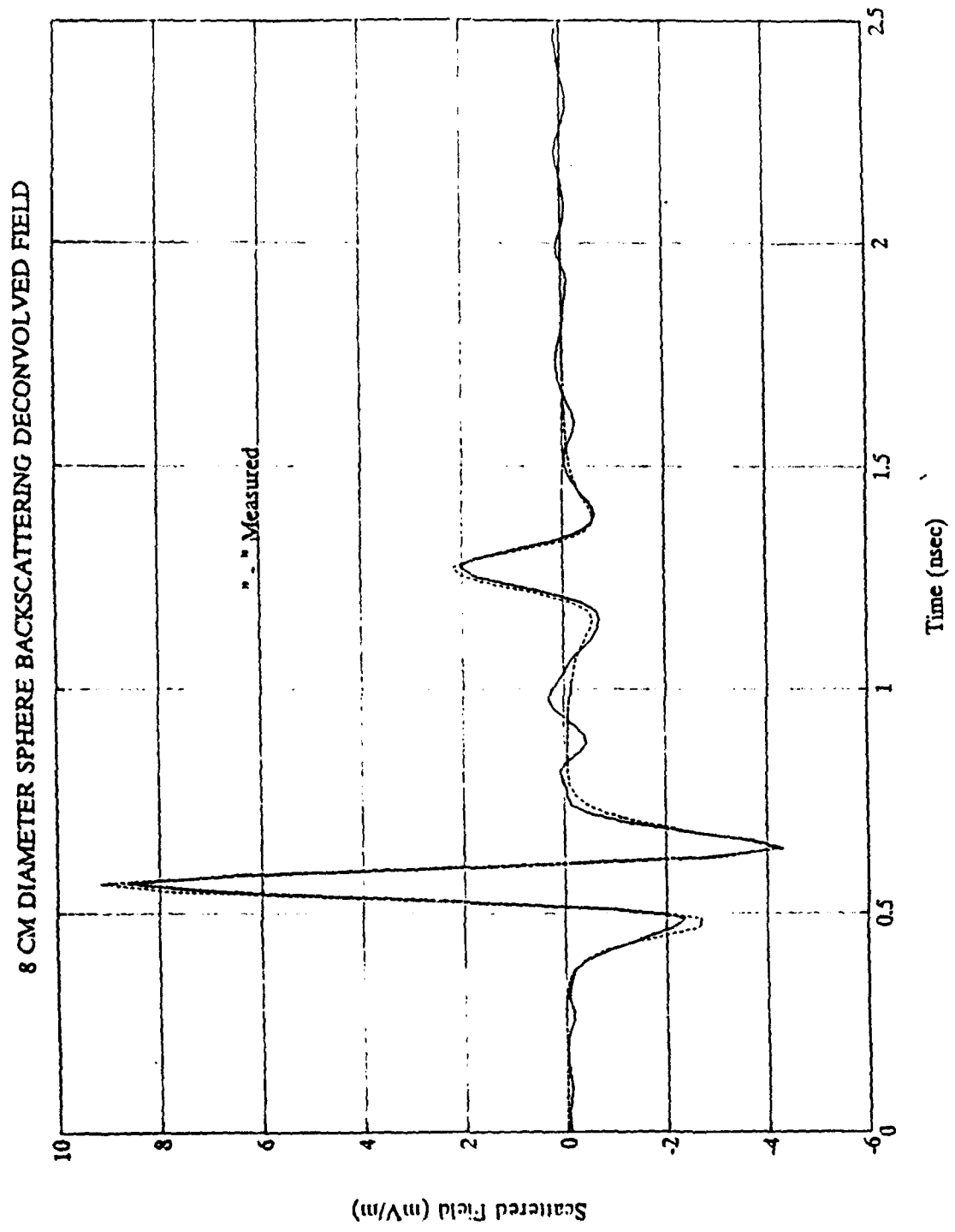


Figure 31. 8 cm Diameter Sphere Validation

D. NOISE PERFORMANCE AND SPECTRUM

The noise performance of the TESL was evaluated by comparing the root mean square (RMS) value of the noise waveforms from old and new configurations. Noise waveforms are formed by subtracting two consecutive background measurements. Although there is record of the old configuration background measurements by Walsh [Ref. 5], two consecutive measurements were not available. Because of this, the noise performance of the updated TESL was calculated using only one background measurement subtracted from the calibration sphere measurement so that the old and new configuration noise performance could be compared during the final 10 Nsec or so of the sampling window, where only noise exists.

Figure 32 shows both subtracted calibration waveforms. This particular window is enlarged and shown in detail in Figure 33.

A Matlab program was written to perform this procedure and calculate the RMS value of both noise waveforms. Due to the limited available data for the old configuration, only a few comparisons could be done. In all cases the new TESL configuration resulted in better noise performance. Figure 33 shows the new configuration RMS value of 0.024 mV compared to the previous setup which yields 0.034 mV.

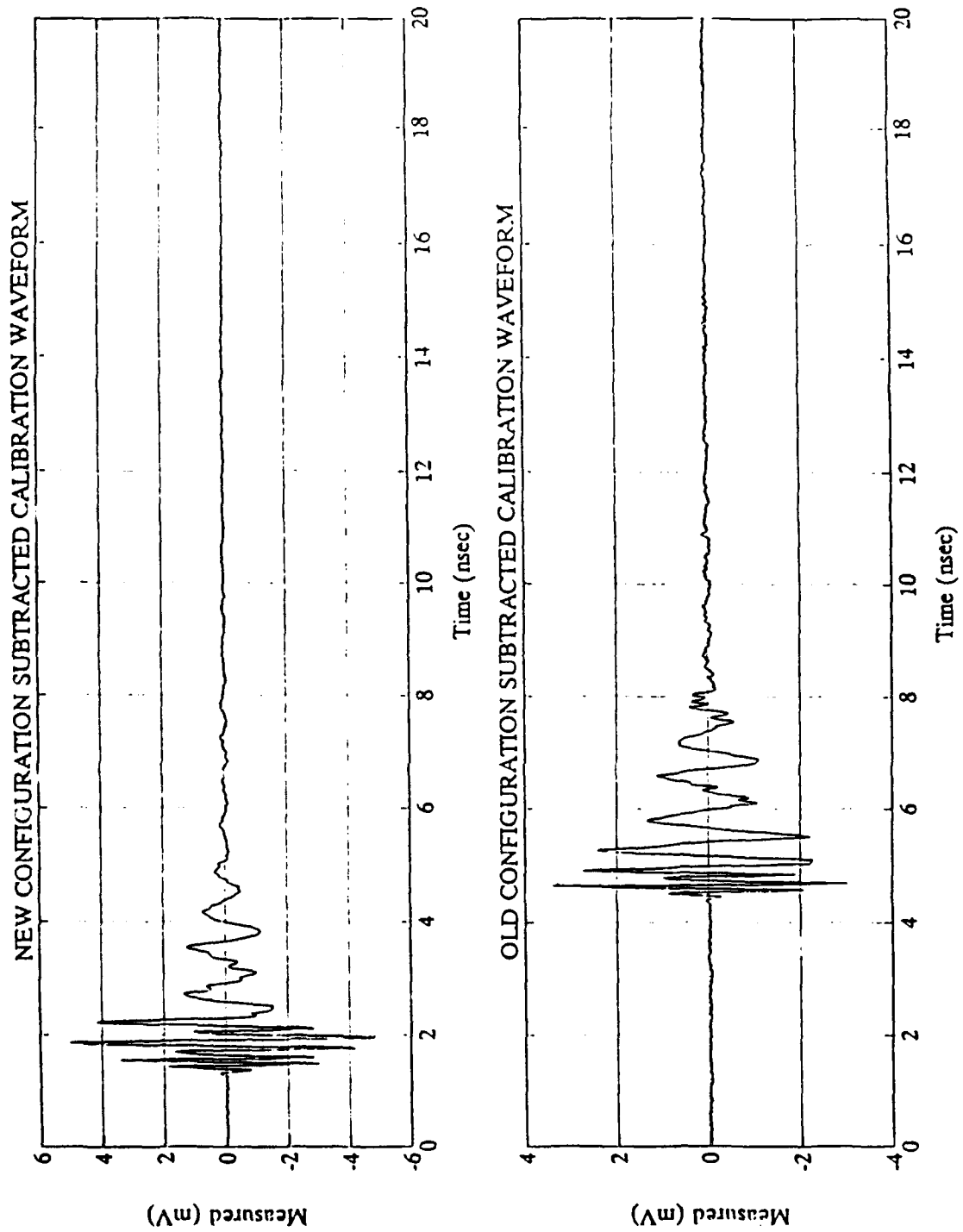


Figure 32. Old and New Configuration Subtracted Calibration Waveforms Considered for the Noise Performance

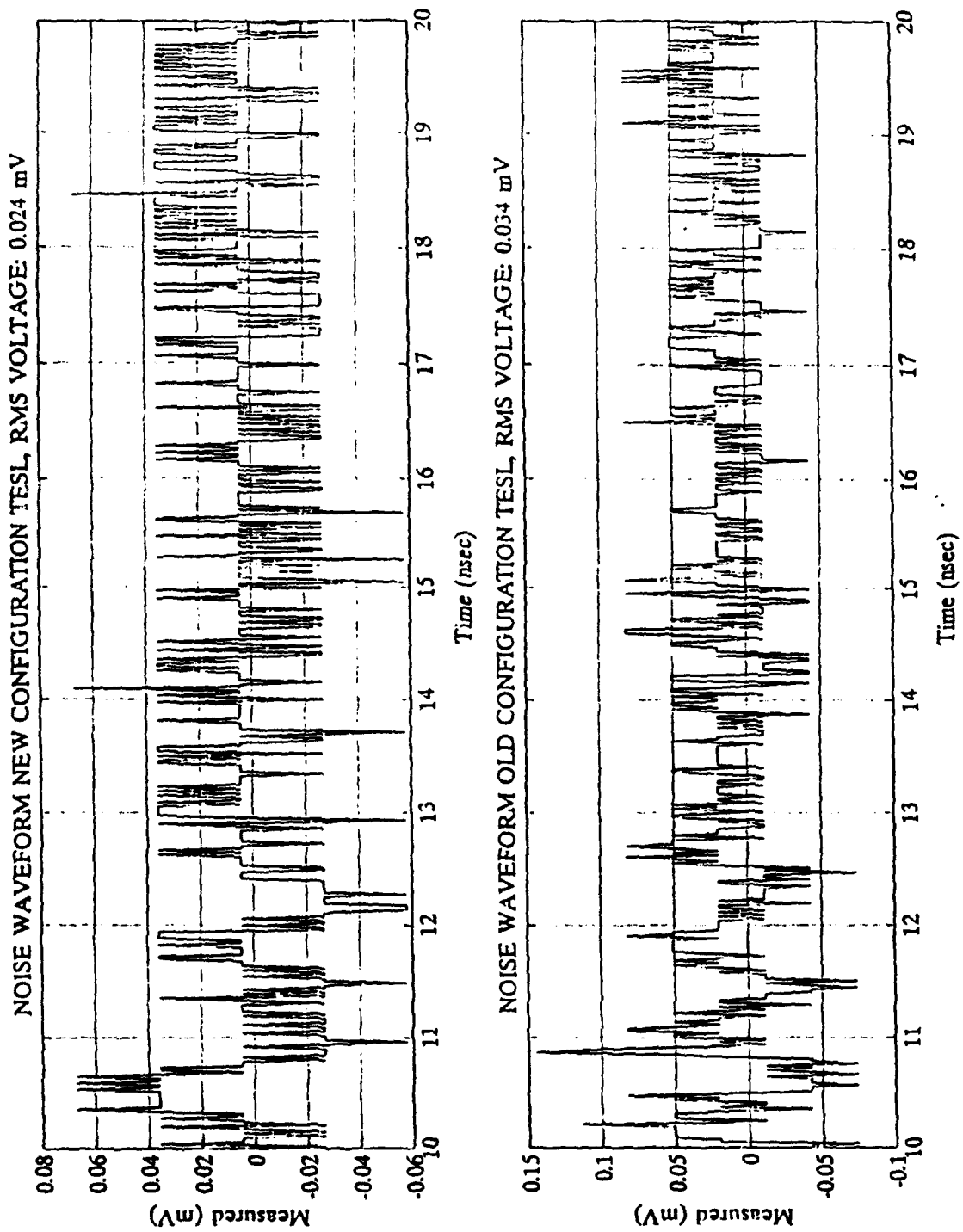


Figure 33. Old and New Configuration Noise Waveforms

Another Matlab program was written to calculate and plot the noise spectrum. The program just requires two consecutive background measurements and asks for the smoothing factor, which is entered by the operator. When a factor of 1 was utilized, the unsmoothed noise spectrum in Figure 34 was obtained. Figure 35 shows the time-smoothed system noise spectrum when a factor of 8 is used.

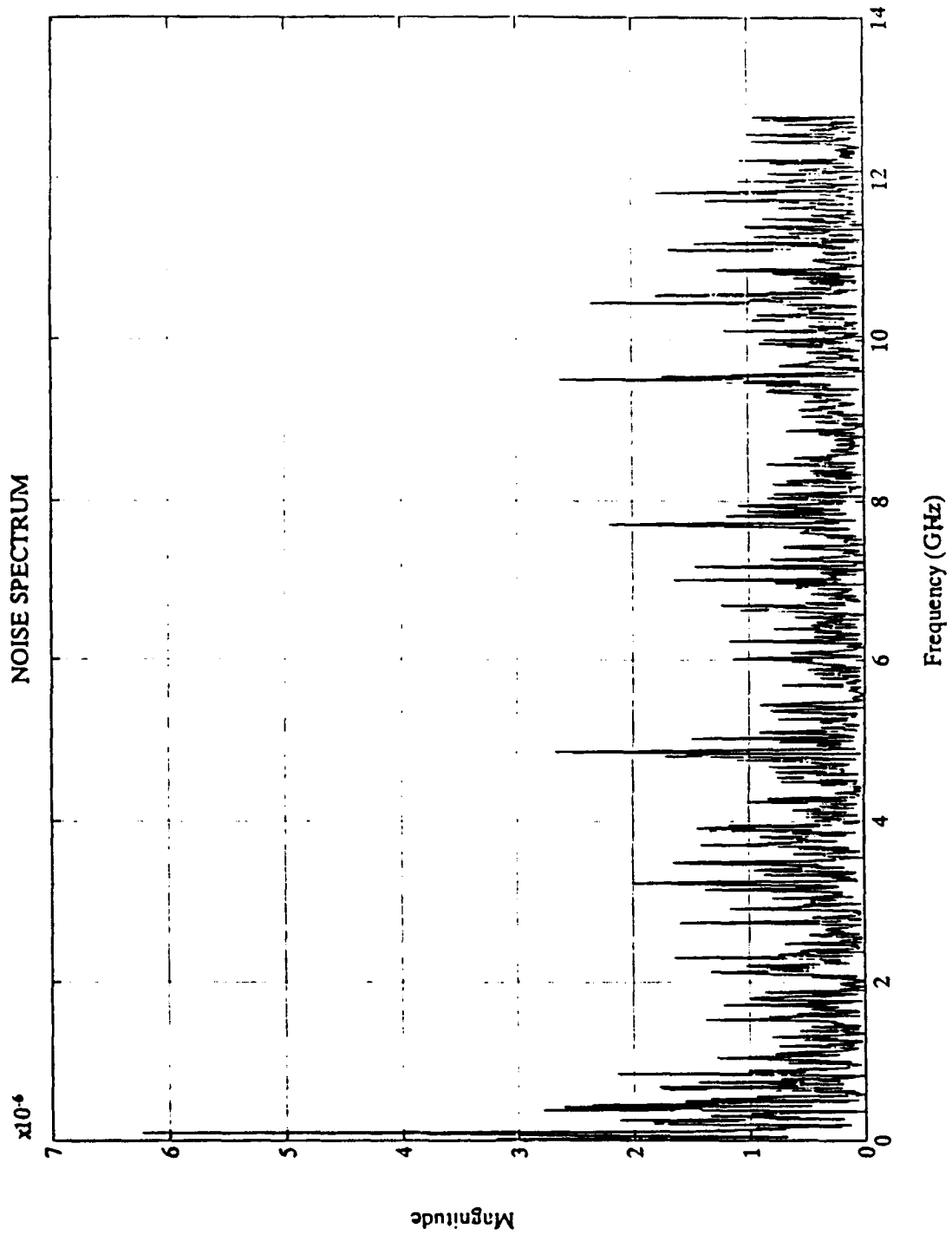


Figure 34. Unsmoothed Noise Spectrum

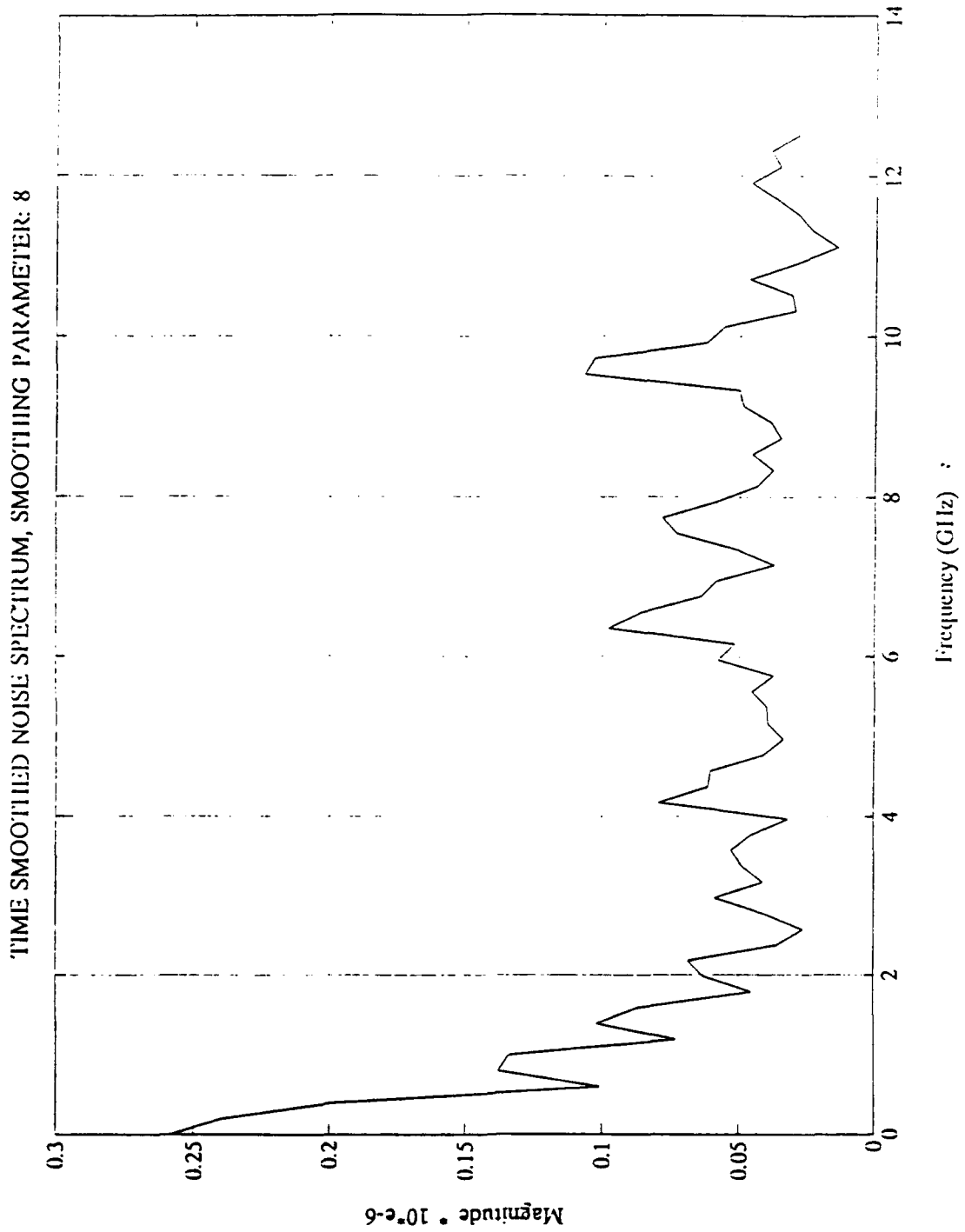


Figure 35. Time Smoothed Noise Spectrum

E. SIGNAL TO NOISE RATIO

A Matlab program was written to calculate the SNR of the TESL. The program begins by asking for the filenames of the measured target waveform and its background. The signal plus noise (denoted by $s(t_k)$) is formed by subtracting this background from the target waveform.

Next, the program asks for the two consecutive background waveforms to estimate the system noise. The noise waveform (denoted by $n(t_k)$) is then formed by subtracting one of these background waveforms from the another. After this, the program presents a message on the screen asking the user to view the record to select the desired time-window which contains only the background signal. When the beginning and the end of the time window have been selected, the program calculates the SNR as shown in equation 4.3.

$$\text{SNR} = 10 \text{ Log} \left[\frac{\sum [s^2(t_k) - n^2(t_k)]}{\sum n^2(t_k)} \right] \quad (4.3)$$

where $s(t_k)$ is the signal plus noise waveform,

$n(t_k)$ is the noise waveform.

McDaniel, Sompase, and Walsh [Refs. 3,4 & 5] calculated the SNR using a 10 cm long and 5.2 mm diameter thick wire as a target in the same way as described in this section. Walsh [Ref. 5] reported a SNR of 26.6 dB with this target. This target was not available when this thesis started. A 10 cm long and 2.36 mm diameter thin wire was used as a target in

order to estimate a comparison with the SNR obtained by the previous work. The same number of points, same number of subaverages and the same acquisition software were used. Although this target is thinner than that used before and a smaller response was expected, the SNR obtained was 30.56 dB using a time-window from 1.9 nsec to 7 nsec, as shown in Figure 36. Different sets of measurements of this thin wire were analyzed, yielding approximately the same SNR. These calculations show that a significant improvement has been achieved in the SNR of the TESL by the results of this work.

F. TARGET LIBRARY

The high level of accuracy of the upgraded TESL has been shown in Section C of this Chapter for simple canonical targets through comparisons with computations. These canonical target validations indicate the accuracy to be expected for complex targets, such as tactical aircraft models, where computations are exceedingly difficult.

A target library was created to support research in aspect invariant radar target identification based on natural resonances. This library contains six files, each one corresponding to a different 1/72 scale model military aircraft which has been coated with silver paint. Each file contains 9 measurements. Each measurement was acquired with the same parameters described in Section A of this Chapter.

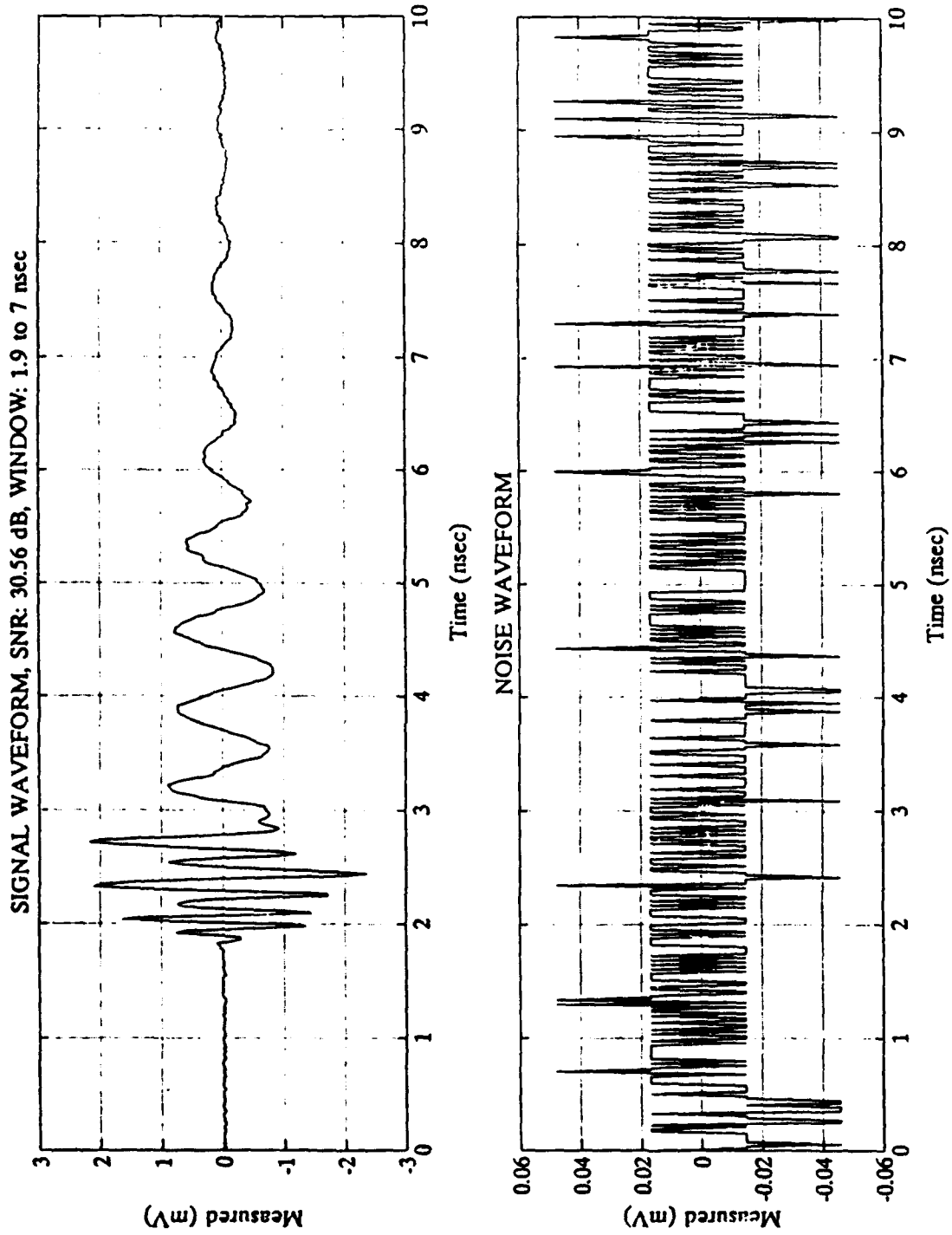


Figure 36. Signal and Noise Waveforms

The 9 measurements for each aircraft are:

- A calibration sphere measurement
- A first background measurement
- A target measurement (0 degrees)
- A second background measurement
- A target measurement (30 degrees)
- A third background measurement
- A target measurement (90 degrees)
- A fourth background measurement
- A target measurement (180 degrees)

The full size dimensions of the aircraft selected are specified in Table 5. Figures 40 and 41 show some of the waveforms obtained.

TABLE 5. AIRCRAFT FULL SIZE DIMENSIONS

Aircraft #	1	2	3	4	5	6
Length (meters)	19.20	16.82	18.85	20.84	20.29	11.15
Height (meters)	4.82	4.60	3.52	4.46	4.32	3.60
Wingspan (meters)	13.10	14.26	10.80	11.52	10.60	9.50
Tailplane (meters)	10.22	5.18	6.40	N/A	5.61	3.31

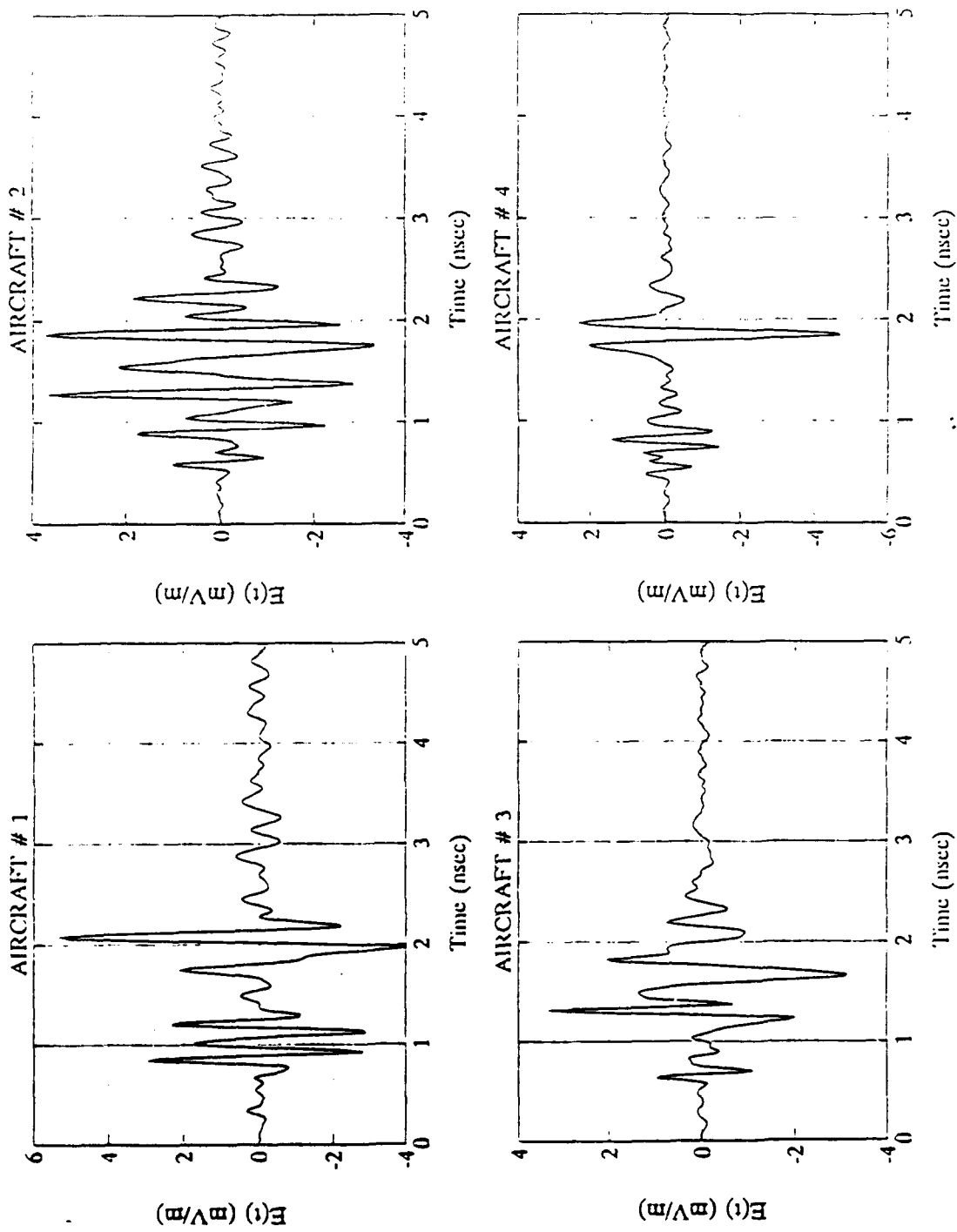


Figure 37. Comparison of Aircraft 1, 2, 3 and 4 Nose-on

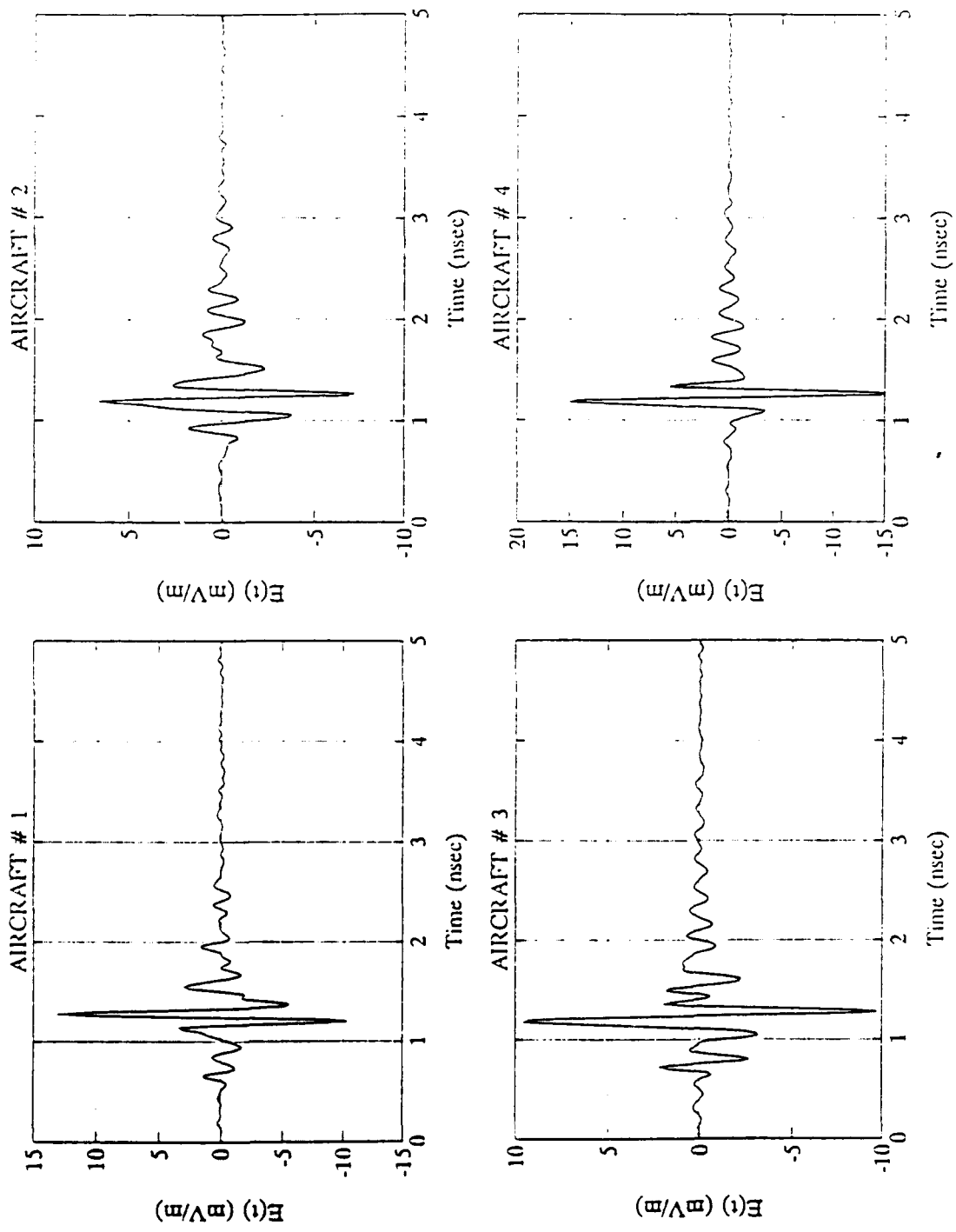


Figure 38. Comparison of Aircraft 1, 2, 3 and 4 Broadside

V. CONCLUSIONS

A. SUMMARY

This thesis describes several improvements obtained by the upgraded TESL. The first stage of this effort was the replacement of the old HP 8349A 2-20 GHz microwave preamplifier with a new Avantek AWT 13533 5-13 GHz (which has a higher gain and a lower noise figure than the HP amplifier). A minimum length coaxial line was used with each amplifier. An undesired oscillation in front of the deconvolved scattered signal for different measured targets was found. The first approach to eliminate the oscillation was directed towards reduction of the quantization of the DPO, without improvement in the final response. Another test was performed taking a set of measurements with a d.c. blocking capacitor installed at the output of the receiving antenna. After deconvolution signal processing, the same undesired response was observed.

A Matlab program was written to evaluate the effect of the delay line in each amplifier. It was found that the delay lines had a large effect in the deconvolved signal. The best results were obtained when the measured waveform from the 2-6 GHz amplifier was delayed 30 time points. It was determined that each shifted time point is equivalent to 4 mm, so an extra 12 cm length delay line for the low frequency amplifier

was needed. With this result, a 25.5 cm delay line was constructed for the 2-6 GHz amplifier, thus giving 13.5 cm corresponding to the minimum delay and 12 cm corresponding to the extra delay. After sets of measurements were taken and processed, the deconvolved signals were validated by comparing with those theoretically predicted. The updated TESL was shown to yield a high level of accuracy.

Additionally, Matlab programs to calculate the SNR, noise spectrum and performance were written and tested. An improvement in the SNR of 4 dB was found, although the reference target was similar but of thinner diameter than the one used in previous experiments.

The final stage in this thesis was the compilation of a high fidelity library for canonical and complex targets. This library will support future research into aspect invariant radar target identification and other scattering experimentation.

B. FUTURE CONSIDERATIONS

Increased SNR can be obtained by replacing the one-watt amplifiers (1-6 GHz and 6-12 GHz) with two-watt amplifiers. Another improvement to the TESL configuration would be mounting all of the hardware in a vertical system rack which will allow higher system flexibility for future modifications.

Since there is a time domain radar target library then it would be worthwhile to create a corresponding frequency domain

library to facilitate complete TESL experimental analysis. Presently there is an ongoing effort in this area which employs a stepped-frequency continuous wave system based on an HP 8510 network analyzer.

APPENDIX A. TIME AND FREQUENCY DOMAIN DECONVOLUTION PROGRAM

The following Matlab program calculates the Deconvolved Field using the Raid's optimal deconvolution estimator as described in chapter IV.

```
% NAME OF THE PROGRAM: DECON.M
% ALGORITHM MADE BY Dr. M.A. MORGAN.
% WRITTEN BY Lt. ALDO E. BRESANI.

% DECONVOLUTION ALGORITHM FOR THE NPS TRANSIENT ELECTROMAGNETIC
% SCATTERING LABORATORY.

% INPUTS ARE THE MEASURED WAVEFORMS, COMPUTED CALIBRATION
% SPHERE AND THE SMOOTHING PARAMETER.
```

```
clg
clear
filename=input('Enter the "Calibration filename".dat to load :','s');
eval(['load ',filename, '.dat'])
data1=eval(filename);
nsav1=data1(1); % NUMBER OF SUBAVERAGES
ntp1 =data1(4); % NUMBER OF TIME POINTS
tstart1=0;
tend1=data1(2);
t1=tend1-tstart1;
['Time window is ',num2str(t1),' nanosec']
['Number of Time Points is ',num2str(ntp1),"]
['Number of subaverages is ',num2str(nsav1),"]
cal=zeros(1,ntp1);
for j=1:ntp1
    cal(j)=data1(j+4);
end ;

filename=input('Enter the "Calibr.Background filename".dat to load :','s');
eval(['load ',filename, '.dat'])
data2=eval(filename);
nsav2=data2(1); % Number of Subaverages
ntp2=data2(4); % Number of Time Points
tstart2=0;
tend2=data2(2);
t2=tend2-tstart2;
['Time window is ',num2str(t2),' nanosec']
['Number of Time Points is ',num2str(ntp2),"]
['Number of subaverages is ',num2str(nsav2),"]
back1=zeros(1,ntp2);
```

```

for j=1:ntp2
    back1(j)=data2(j+4);
end ;
ntp=ntp1;
dt=t1/(ntp-1);
t=0:dt:tend1;    % DEFINING TIME AXIS
f=((ntp/(2*t1))/ntp)*(0:ntp-1);    % DEFINING FREQUENCY AXIS
dt2=10/511;
t2=0:dt2:10;
dt1=5/255;
T1=0:dt1:5;
ycal=zeros(1,ntp);
for k=1:ntp
    ycal(k)=cal(k)-back1(k);
end;

subplot(211),plot(t2,(1000.*(cal(1:512))),'-r',.....
.....t2,(1000.*(back1(1:512))), '--g')
title('CALIBRATION AND BACKGROUND WAVEFORM');
xlabel('Time (nsec)');
grid;
ylabel('Measured (mV)');
pause;

subplot(212),plot(t2,(1000.*(ycal(1:512))))
title('SUBTRACTED CALIBRATION WAVEFORM');
xlabel('Time (nsec)');
grid;
ylabel('Measured (mV)');
meta lica;
pause;
clg;

Ycal = fft(ycal,2*ntp);

plot(f,(1000*abs(Ycal(1:ntp))))
title('CALIBRATION SPECTRUM');
xlabel('Frequency (GHz)');
grid;
ylabel('Magnitude');
meta lica;
pause;
clg ;

filename=input('Enter the "Target filename".dat to load :','s');
eval(['load ',filename,'.dat'])
data3=eval(filename);
nsav3=data3(1);    % Number of Subaverages
ntp3=data3(4);    % Number of Time Points
tstart3=0;
tend3=data3(2);

```

```

t3=tend3-tstart3;
['Time window is ',num2str(t3),' nanosec']
['Number of Time Points is ',num2str(ntp3),"]
['Number of subaverages is ',num2str(nsav3),"]
targ=zeros(1,ntp3);
for j=1:ntp3
    targ(j)=data3(j+4);
end ;

h=input('Do you want to use the same Back. file (0 for N, 1 for Y): ');

if h==0

filename=input('Enter the "Targ.Background filename".dat to load.... ....','s'),
eval(['load ',filename, '.dat'])
data5=eval(filename);
nsav5=data5(1); % Number of Subaverages
ntp5=data5(4); % Number of Time Points
tstart5=0;
tend5=data5(2);
t5=tend5-tstart5;
['Time window is ',num2str(t5),' nanosec']
['Number of Time Points is ',num2str(ntp5),"]
['Number of subaverages is ',num2str(nsav5),"]
back2=zeros(1,ntp5);
for j=1:ntp5
    back2(j)=data5(j+4);
end ;

else
    back2=zeros(1,ntp);
    for j=1:ntp2
        back2(j)=back1(j);
    end;
end;

ysct=zeros(1:ntp);
for k=1:ntp
    ysct(k)=targ(k)-back2(k);
end;

subplot(211),plot(t2,(1000.*(targ(1:512))),'-r',.....
.....t2,(1000.*(back2(1:512))),'-g')
title('TARGET AND BACKGROUND WAVEFORM');
xlabel('Time (nsec)');
ylabel('Measured (mV)');
grid;
pause;

subplot(212),plot(t2,(1000.*(ysct(1:512))))
title('SUBTRACTED TARGET WAVEFORM');

```

```

xlabel('Time (nsec)');
ylabel('Measured (mV)');
grid;
meta lica;
pause;
clg;

```

```

Ysct = fft(ysct,2*ntp);

```

```

plot(f,(1000*abs(Ysct(1:ntp))))
title('Target Spectrum');
xlabel('Frequency (GHz)');
ylabel('Magnitude');
grid;
meta lica;
pause;
clg ;

```

```

filename=input('Enter the "Computed Sphere filename".dat to load.... ....','s');
eval(['load ',filename,'.dat'])
data4=eval(filename);
ntp4=data4(1); % Number of Time Points
tstart4=data4(2);
tend4=data4(3);
t4=tend4-tstart4;
['Time window is ',num2str(t4),' nanosec']
['Number of Time Points is ',num2str(ntp4),"]
ycom=zeros(1,ntp4);
for j=1:ntp4
    ycom(j)=data4(j+3);
end ;

```

```

l=input('Enter the smoothing factor :');

```

```

Ylcal= conj(Ycal) ;
a=0;
for n=1:2*ntp
    a=a+(abs(Ycal(n))).^2 ;
end;
b=a/(ntp);
c=(l)^2;
d=c*b;
Z=zeros(1,2*ntp) ;

```

```

for n=1:(2*ntp)
Z(n)=(Ysct(n).*Ylcal(n))./((abs(Ycal(n)))^2+d);% DECOVOLUTION COMPONENT
end;
z=zeros(1,2*ntp) ;
z=ifft(Z,2*ntp) ; % DECONVOLVED IMPULSE RESPONSE
Ycom=fft(ycom,2*ntp) ;

```

```

s3=Ycom.*conj(Ycom) ; % SPECTRUM COMPUTED CALIBRATION SPHERE
subplot(211),plot(T1,(1000.*ycom(1:256))) ; grid
title('COMPUTED SPHERE SCATTERED E(t) IN mV/m');
xlabel('Time (nsec)');
pause;

subplot(212),plot(f,(1000.*real(s3(1:ntp))))
grid;
title('COMPUTED SPHERE SCATTERED SPECTRUM |E(f)|');
xlabel('Frequency (GHz)');
meta lica;
pause;
clg;
ZZ=Z.*Ycom ;

% FREQUENCY DOMAIN DECONVOLUTION

zz=ifft(ZZ,2*ntp);

plot(f,(1000.*abs(Z(1:ntp)))) ;
title('DECONVOLUTION COMPONENT');
grid;
xlabel('Frequency (GHz)');
meta lica;
pause;
clg

plot(f,(1000.*abs(ZZ(1:ntp))))
title(['DECONVOLUTION SPECTRUM, SMOOTHING: ',num2str(1)]);
xlabel('Frequency (GHz)');
ylabel('Magnitude');
grid;
meta lica;
pause;
clg

plot(T1,(1000.*real(zz(1:256))))
title(['DECONVOLVED FIELD, SMOOTHING: ',num2str(1)]);
xlabel('Time (nsec)');
ylabel('E(t) (mV/m)');
grid;
meta lica;
pause;
clg

% TIME DOMAIN DECONVOLUTION

cc=conv(z(1:256),ycom(1:256));
subplot(211),plot(T1,(1000.*ycom(1:256))) ; grid
title('COMPUTED SPHERE SCATTERED E(t) IN mV/m');

```

```
xlabel('Time (nsec)');
pause;
subplot(212),plot(T1,(1000.*real(z(1:256)))) ;
title(['DECONVOLVED IMPULSE RESPONSE, SMOOTHING: ',num2str(l)]);
xlabel('Time (nsec)');
grid;
meta lica;
pause;
clg;

plot(T1,(1000.*(cc(1:256)))) ;
title(['HYBRID DECONVOLVED FIELD, SMOOTHING: ',num2str(l)]);
xlabel('TIME (nsec)');
ylabel('SCAT.E-FIELD(mV/m)');
grid;
meta lica;
pause;
end;
```

APPENDIX B. DELAY LINE SIMULATION PROGRAM

The following Matlab program simulates the effect of the delay line in each of the amplifiers of the TESL.

```
% NAME OF THE PROGRAM: SIMDEL.M
% WRITTEN BY Lt. ALDO E. BRESANI

% INPUTS ARE THE MEASURED WAVEFORMS, COMPUTED CALIBRATION
% SPHERE AND THE SMOOTHING PARAMETER.

clg
clear

q=input('Enter the shift for 1-6 GHz ');

filename=input('Enter the "Calibration 1-6 GHz".dat to load :','s');
eval(['load ',filename,'.dat'])
data1=eval(filename);
ntp1 =data1(4); % NUMBER OF TIME POINTS
tstart1=0;
tend1=data1(2);
t1=tend1-tstart1;
call=zeros(1,ntp1);
for j=1:ntp1
    call(j)=data1(j+4);
end ;
call1=zeros(1:1024);
for k=1:q
    call1(k)=0;
end;
for k=(q+1):1024
    call1(k)= call(k-q);
end;

filename=input('Enter the "Calibr.Background 1-6 GHz".dat to load :','s');
eval(['load ',filename,'.dat'])
data2=eval(filename);
ntp2=data2(4); % Number of Time Points
tstart2=0;
tend2=data2(2);
t2=tend2-tstart2;
back1=zeros(1,ntp2);
for j=1:ntp2
    back1(j)=data2(j+4);
end ;
```

```

back11=zeros(1:1024);
for k=1:q
    back11(k)=0;
end;
for k=q+1:1024
    back11(k)= back1(k-q);
end;

ntp=ntp1;
dt=t1/(ntp-1);
t=0:dt:tend1; % DEFINING TIME AXIS
f=((ntp/(t1))/ntp)*(0:ntp/2-1); % DEFINING FREQUENCY AXIS
dt2=10/511;
t2=0:dt2:10;
dt1=5/255;
T1=0:dt1:5;

ycall=zeros(1,ntp);
for k=1:ntp
    ycall(k)=call1(k)-back11(k);
end;

subplot(211),plot(t2,(1000.*(call1(1:512))),'-r',.....
.....t2,(1000.*(back11(1:512))),'-g')
title('CALIBRATION AND BACKGROUND WAVEFORM');
xlabel('Time (nsec)');
ylabel('Measured (mV)');
grid;
pause;

subplot(212),plot(t2,(1000.*(ycall(1:512))))
title('SUBTRACTED CALIBRATION WAVEFORM');
xlabel('Time (nsec)');
ylabel('Measured (mV)');
grid;
pause;
clf;

filename=input('Enter the "Calibration 6-12 GHz".dat to load :','s');
eval(['load ',filename,'.dat'])
data10=eval(filename);
ntp10 =data10(4); % NUMBER OF TIME POINTS
tstart10=0;
tend10=data10(2);
t10=tend10-tstart10;
cal2=zeros(1,ntp10);
for j=1-ntp10
    cal2(j)=data10(j+4);
end ;

filename=input('Enter the "Calibr.Background 6-12 GHz".dat to load.... :','s');

```

```

eval(['load ',filename,'.dat'])
data20=eval(filename);
ntp20=data20(4);    % Number of Time Points
tstart20=0;
tend20=data20(2);
t20=tend20-tstart20;
back2=zeros(1,ntp20);
for j=1:ntp20
    back2(j)=data20(j+4);
end ;

ycall2=zeros(1:ntp);
for k=1:ntp
    ycall2(k)=cal2(k)-back2(k);
end;

subplot(211),plot(t2,(1000.*(cal2(1:512))),'-r',.....
.....t2,(1000.*(back2(1:512))),'-g')
title('CALIBRATION AND BACKGROUND 6-12');
xlabel('Time (nsec)');
ylabel('Measured (mV)');
grid;
pause;

subplot(212),plot(t2,(1000.*(ycall2(1:512))))
title('SUBTRACTED CALIBRATION WAVEFORM');
xlabel('Time (nsec)');
ylabel('Measured (mV)');
grid;
pause;
clf;

for k=1:1024
    ycal(k)=ycall(k)+ycall2(k);
end;
for n=513:1024
    ycal(n)=0;
end;
Ycal = fft(ycal,ntp);

plot(f,(1000*abs(Ycal(1:ntp/2))))
title('Calibration Spectrum');
xlabel('Frequency (GHz)');
grid;
pause;
clf ;

filename=input('Enter the "Target 1-6 GHz".dat to load :','s');
eval(['load ',filename,'.dat'])
data3=eval(filename);
ntp3=data3(4);    % Number of Time Points

```

```

tstart3=0;
tend3=data3(2);
t3=tend3-tstart3;
targ1=zeros(1,ntp3);
for j=1:ntp3
    targ1(j)=data3(j+4);
end ;

targ11=zeros(1:1024);
for k=1:q
    targ11(k)=0;
end;

for k=q+1:1024
    targ11(k)= targ1(k-q);
end;

filename=input('Enter the "Target 6-12 GHz".dat to load :','s');
eval(['load ',filename,'.dat'])
data30=eval(filename);
ntp30=data30(4); % Number of Time Points
tstart30=0;
tend30=data30(2);
t30=tend30-tstart30;
targ2=zeros(1,ntp30);
for j=1:ntp30
    targ2(j)=data30(j+4);
end ;

ysct1=zeros(1:ntp);
ysct2=zeros(1:ntp);

for k=1:ntp
    ysct1(k)=targ11(k)-back11(k);
    ysct2(k)=targ2(k)-back2(k);
end;

ysct=zeros(1:ntp);

for k=1:ntp
    ysct(k)=ysct1(k)+ysct2(k);
end;

subplot(211),plot(t2,(1000.*(targ11(1:512))),'-r',.....
.....t2,(1000.*(back11(1:512))),'-g')
title('TARGET AND BACKGROUND 1-6 GHz');
xlabel('Time (nsec)');
ylabel('Measured (mV)');
grid;
pause;

```

```

subplot(212),plot(t2,(1000.*(ysct1(1:512))))
title('SUBTRACTED TARGET WAVEFORM');
xlabel('Time (nsec)');
ylabel('Measured (mV)');
grid;
pause;
clg;

subplot(211),plot(t2,(1000.*(targ2(1:512))),'-r',.....
.....t2,(1000.*(back2(1:512))),'--g')
title('TARGET AND BACKGROUND 6-12 GHz');
xlabel('Time (nsec)');
ylabel('Measured (mV)');
grid;
pause;

subplot(212),plot(t2,(1000.*(ysct2(1:512))))
title('SUBTRACTED TARGET WAVEFORM');
xlabel('Time (nsec)');
ylabel('Measured (mV)');
grid;
pause;
clg;

Ysct = fft(ysct,ntp);

plot(f,(1000*abs(Ysct(1:ntp/2))))
title('Target Spectrum');
xlabel('Frequency (GHz)');
grid;
pause;
clg ;

filename=input('Enter the "Computed Sphere filename".dat to load.... .....','s');
eval(['load ',filename,'.dat'])
data4=eval(filename);
ntp4=data4(1); % Number of Time Points
tstart4=data4(2);
tend4=data4(3);
t4=tend4-tstart4;
['Time window is ',num2str(t4),' nanosec']
['Number of Time Points is ',num2str(ntp4),']
ycom=zeros(1,ntp4);
for j=1:ntp4
    ycom(j)=data4(j+3);
end ;

cc=conv(ysct,ycom);
gg=zeros(1,ntp);
for n=1:1023
    gg(n)=cc(n);

```

```

end;
gg(1024)=0;
GG=fft(gg,ntp);

l=input('Enter the smoothing factor :');
Y1cal= conj(Ycal) ;
a=0
for n=1:ntp
    a=a+(abs(Ycal(n))).^2 ;
end;
b=a/(ntp);

c=(l)^2
d=c*b;
Z=zeros(1,ntp) ;
for n=1:ntp
    Z(n)=(GG(n).*Y1cal(n))./((abs(Ycal(n)))^2+d) ;
end;

plot(f,(1000.*abs(Z(1:ntp/2))))
title(['DECONVOLUTION SPECTRUM, SMOOTHING: ',num2str(l)]);
xlabel('Frequency (GHz)');
ylabel('Magnitude');
grid;
meta sim;
pause;
clg

z=zeros(1,ntp) ;
z=ifft(Z,ntp) ;

plot(T1,real(z(1:256)))
title(['DECONVOLVED FIELD, SMOOTHING: ',num2str(l)]);
xlabel('Time (nsec)');
ylabel('E(t) (mV/m)');
grid;
meta sim;
pause;

```

APPENDIX C. SNR AND NOISE SPECTRUM PROGRAM

The following Matlab program calculates the signal to noise ratio and the noise spectrum of the TESL.

```
% NAME OF THE PROGRAM: SNR.M
% WRITTEN BY Lt. ALDO E. BRESANI

% THIS PROGRAM CALCULATES THE SIGNAL TO NOISE RATIO FOR THE
% TRANSIENT ELECTROMAGNETIC SCATTERING LABORATORY, AND THE
% SYSTEM NOISE SPECTRUM.

% INPUTS ARE THE TARGET MEASUREMENT AND ITS BACKGROUND, AND
% TWO CONSECUTIVE BACKGROUND MEASUREMENTS.

clg
clear
filename=input('Enter the "Target filename".dat to load :','s');
eval(['load ',filename,'.dat'])
data1=eval(filename);
nsav1=data1(1); % NUMBER OF SUBAVERAGES
ntp1 =data1(4); % NUMBER OF TIME POINTS
tstart1=0;
tend1=data1(2);
t1=tend1-tstart1;
['Time window is ',num2str(t1),' nanosec']
['Number of Time Points is ',num2str(ntp1),"]
['Number of subaverages is ',num2str(nsav1),"]
targ=zeros(1,ntp1);
for j=1:ntp1
    targ(j)=data1(j+4);
end;

filename=input('Enter the "Target Backg. filename".dat to load :','s');
eval(['load ',filename,'.dat'])
data4=eval(filename);
nsav4=data4(1); % Number of Subaverages
ntp4=data4(4); % Number of Time Points
tstart4=0;
tend4=data4(2);
t4=tend4-tstart4;
['Time window is ',num2str(t4),' nanosec']
['Number of Time Points is ',num2str(ntp4),"]
['Number of subaverages is ',num2str(nsav4),"]
back0=zeros(1,ntp4);
for j=1:ntp4
```

```

    back0(j)=data4(j+4);
end ;

filename=input('Enter the "Background1 filename".dat to load :','s');
eval(['load ',filename,'.dat'])
data2=eval(filename);
nsav2=data2(1); % Number of Subaverages
ntp2=data2(4); % Number of Time Points
tstart2=0;
tend2=data2(2);
t2=tend2-tstart2;
['Time window is ',num2str(t2),' nanosec']
['Number of Time Points is ',num2str(ntp2),"]
['Number of subaverages is ',num2str(nsav2),"]
back1=zeros(1,ntp2);
for j=1:ntp2
    back1(j)=data2(j+4);
end ;

filename=input('Enter the "Background2 filename".dat to load :','s');
eval(['load ',filename,'.dat'])
data3=eval(filename);
nsav3=data3(1); % Number of Subaverages
ntp3=data3(4); % Number of Time Points
tstart3=0;
tend3=data3(2);
t3=tend3-tstart3;
['Time window is ',num2str(t3),' nanosec']
['Number of Time Points is ',num2str(ntp3),"]
['Number of subaverages is ',num2str(nsav3),"]
back2=zeros(1,ntp3);
for j=1:ntp3
    back2(j)=data3(j+4);
end ;

% FORMING THE SIGNAL AND NOISE POWER

ntp=ntp1;
s=zeros(1,ntp);
n=zeros(1,ntp);
n1=zeros(1,ntp);

('You will see the signal waveform. Please note the window desired.')

for k=1:ntp
    s(k)=targ(k)-back0(k);
    n(k)=back1(k)-back2(k);
end;

% DEFINING TIME AXIS

```

```

dt2=10/511;
t2=0:dt2:10;

plot(t2,(1000.*(s(1:512))))
title('SIGNAL WAVEFORM');
xlabel('Time (nsec)');
ylabel('Measured (mV/m)');
grid;
pause;
clf;

x=input('Enter the begining for time window: ')
y=input('Enter the end for time window: ')

x1=x/0.01953125 ;
y1=y/0.01953125 ;
sum1=0;
sum2=0;
for k=x1:y1
    sum1=sum1+(s(k).^2)-(n(k).^2);
    sum2=sum2+(n(k).^2);
end;

% FORMING THE SIGNAL TO NOISE RATIO

snr=sum1/sum2;
SNR=10.*log10(snr);

% DEFINING TIME AXIS

dt=t1/(ntp-1);
t=0:dt:tend1;
dt1=5/255;
T1=0:dt1:5;

subplot(211),plot(t2,(1000.*(s(1:512))))
title(['SIGNAL WAVEFORM, SNR: ',num2str(SNR),' dB, WINDOW:.....
..... ',num2str(x),' to ',num2str(y),' nsec']);
xlabel('Time (nsec)');
ylabel('Measured (mV)');
grid;
pause;

subplot(212),plot(t2,(1000.*(n(1:512))))
title('NOISE WAVEFORM');
xlabel('Time (nsec)');
ylabel('Measured (mV)');
grid
meta snr;
pause;
clf;

```

```

% NOISE SPECTRUM

k=input('Enter the smoothing parameter for noise spectrum: ')

M=ntp/k;
f=(1/(4*t1))*(0:ntp-1);

% UNSMOOTHED NOISE SPECTRUM

n1=xcorr(n);
N=fft(n1,2*ntp);

plot(f,abs(N(1:ntp)));
grid;
xlabel('Frequency (GHz)');
ylabel('Magnitude');
title('NOISE SPECTRUM');
meta snr;
pause;

% TIME SMOOTHED NOISE SPECTRUM

H=zeros(1,M);
for i=1:k
    l(i,:)=n((1+(i-1)*M):i*M);
    q1(i,:)=xcorr(l(i,:));
    q(i,:)=fft(q1(i,:),2*M);
end;
H=sum(q)/k;
f1=(12.5/(M/2-1))*(0:(M/2-1));

plot(f1,1000000.*real(H(1:M/2)));
xlabel('Frequency (GHz)');
ylabel('Magnitude * 10^e-6');
title(['TIME SMOOTHED NOISE SPECTRUM, SMOOTHING PARAMETER:....',
.... ',num2str(k)']);
grid;
meta snr;
pause;

```

APPENDIX D. NOISE PERFORMANCE PROGRAM

The following Matlab program makes a noise performance comparison between the old and new configuration of the TESL.

```
% NAME OF THE PROGRAM: NOISE.M
% WRITTEN BY Lt. ALDO E. BRESANI

% THIS PROGRAM EVALUATES THE NOISE PERFORMANCE FOR THE
% TRANSIENT ELECTROMAGNETIC SCATTERING LABORATORY. IT MAKES
% A COMPARISON BETWEEN OLD AND NEW CONFIGURATION.

% INPUTS ARE THE CALIBRATION MEASUREMENTS AND THEIR
% BACKGROUNDS

clg
clear
filename=input('Enter the "New Config.Cal.filename".dat to load.... ....','s');
eval(['load ',filename,'.dat'])
data1=eval(filename);
nsav1=data1(1); % Number of Subaverages
ntp1 =data1(4); % Number of Time Points
tstart1=0;
tend1=data1(2);
t1=tend1-tstart1;
['Time window is ',num2str(t1),' nanosec']
['Number of Time Points is ',num2str(ntp1),"]
['Number of subaverages is ',num2str(nsav1),"]
cal1=zeros(1,ntp1);
for j=1:ntp1
    cal1(j)=data1(j+4);
end ;
filename=input('Enter the "Old Config.Cal.filename".dat to load.... ....','s');
eval(['load ',filename,'.dat'])
data2=eval(filename);
nsav2=data2(1); % Number of Subaverages
ntp2=data2(4); % Number of Time Points
tstart2=0;
tend2=data2(2);
t2=tend2-tstart2;
['Time window is ',num2str(t2),' nanosec']
['Number of Time Points is ',num2str(ntp2),"]
['Number of subaverages is ',num2str(nsav2),"]
cal2=zeros(1,ntp2);
for j=1:ntp2
    cal2(j)=data2(j+4);
end ;
```

```

filename=input('Enter the "New Config.Back.filename".dat to load.... .....','s');
eval(['load ',filename,'.dat'])
data3=eval(filename);
nsav3=data3(1); % Number of Subaverages
ntp3=data3(4); % Number of Time Points
tstart3=0;
tend3=data3(2);
t3=tend3-tstart3;
['Time window is ',num2str(t3),' nanosec']
['Number of Time Points is ',num2str(ntp3),"]
['Number of subaverages is ',num2str(nsav3),"]
back1=zeros(1,ntp3);
for j=1:ntp3
    back1(j)=data3(j+4);
end ;

filename=input('Enter the "Old Config.Back.filename".dat to load.... .....','s');
eval(['load ',filename,'.dat'])
data4=eval(filename);
nsav4=data4(1); % Number of Subaverages
ntp4=data4(4); % Number of Time Points
tstart4=0;
tend4=data4(2);
t4=tend4-tstart4;
['Time window is ',num2str(t4),' nanosec']
['Number of Time Points is ',num2str(ntp4),"]
['Number of subaverages is ',num2str(nsav4),"]
back2=zeros(1,ntp4);
for j=1:ntp4
    back2(j)=data4(j+4);
end ;

ntp=ntp1;
sub1=zeros(1,ntp);
sub2=zeros(1,ntp);
for k=1:1024
    sub1(k)=cal1(k)-back1(k);
    sub2(k)=cal2(k)-back2(k);
end;

sum1=0;
for j=513:1024
    sum1=sum1+(sub1(j))^2;
end
x=sum1/512;
rmsn=(x)^.5;
rmsn1=1000*rmsn;

sum2=0;
for j=513:1024
    sum2=sum2+(sub2(j))^2;

```

```

end
y=sum2/512;
rmso=(y)^.5;
rmsol=1000*rmso;
dt=t1/(ntp-1);

%   DEFINING TIME AXIS

t=0:dt:tend1;
dt1=5/255;
T1=0:dt1:5;
dt2=10/511;
t2=10:dt2:20;

subplot(211),plot(t,(1000.*(sub1)))
title('NEW CONFIGURATION SUBTRACTED CALIBRATION WAVEFORM');
xlabel('Time (nsec)');
ylabel('Measured (mV)');
grid
pause;

subplot(212),plot(t,(1000.*(sub2)))
title('OLD CONFIGURATION SUBTRACTED CALIBRATION WAVEFORM');
xlabel('Time (nsec)');
ylabel('Measured (mV)');
grid
meta noise;
pause;
clg

subplot(211),plot(t2,(1000.*(sub1(513:1024))))
title(['NOISE WAVEFORM NEW CONFIGURATION TESL,.....
..... RMS VOLTAGE: ',num2str(rmsn1),' mV']);
xlabel('Time (nsec)');
ylabel('Measured (mV)');
grid
pause;

subplot(212),plot(t2,(1000.*(sub2(513:1024))))
title(['NOISE WAVEFORM OLD CONFIGURATION TESL,.....
..... RMS VOLTAGE: ',num2str(rmsol),' mV']);
xlabel('Time (nsec)');
ylabel('Measured (mV)');
grid
meta noise;
pause;
clg
end

```

LIST OF REFERENCES

1. C.W. Hammond, "The Development of a Bistatic Electromagnetic Scattering Laboratory", Master's Thesis, Naval Postgraduate School, Monterey, CA, 1980.
2. M.A. Mariategui, "Development, Calibration, and Evaluation of a Free Field Scattering Range", Master's Thesis, Naval Postgraduate School, Monterey, CA, 1983.
3. B.W. McDaniel, "Calibration and Evaluation of a Free Field Scattering Range Using Wideband Pulse Amplification", Master's Thesis, Naval Postgraduate School, Monterey, CA, 1985.
4. Soonpuen Sompae, "Computer Algorithms For Measurement, Control, and Signal Processing of Transient Scattering Signatures", Master's Thesis, Naval Postgraduate School, Monterey, CA, 1988.
5. Norman J. Walsh, "Bandwidth and Signal to Noise Ratio Enhancement of The NPS Transient Electromagnetic Scattering Laboratory", Master's Thesis, Naval Postgraduate School, Monterey, CA, 1989.
6. S.M. Raid, "Impulse Response Evaluation Using Frequency Domain Optimal Compensation Deconvolution", presented at the Midwest Symposium on Circuits and Systems, University of Toledo, OH, August 1981.

INITIAL DISTRIBUTION LIST

	No Copies
1. Defense Technical Information Center Cameron Station Alexandria, VA 22304-6145	2
2. Library, Code 52 Naval Postgraduate School Monterey, CA 93943-5002	2
3. Department Chairman, Code EC Department of Electrical and Computer Engineering Naval Postgraduate School Monterey, CA 93943-5100	1
4. Group Chairman, Code EW Naval Postgraduate School Monterey, CA 93943-5000	1
5. Professor M. A. Morgan, Code EC/Mw Department of Electrical and Computer Engineering Naval Postgraduate School Monterey, CA 93943-5100	6
6. Professor J. B. Knorr, Code EC/Ko Department of Electrical and Computer Engineering Naval Postgraduate School Monterey, CA 93943-5100	1
7. Professor R. Janaswamy, Code EC/Js Department of Electrical and Computer Engineering Naval Postgraduate School Monterey, CA 93943-5100	1
8. LT A. E. Bresani Embassy of Peru Naval Attache Office 2160 Wisconsin Ave. N.W. Washington D.C. 20007	1